Survey: Characterization and Mitigation of Spatial/Spectral Interferers and Transceiver Nonlinearities for 5G MIMO Systems

Nicholas Peccarelli, *Student Member, IEEE,* Blake James, *Student Member, IEEE*
Robin Irazoqui, *Student Member, IEEE,* Justin Metcalf, *Member, IEEE* Caleb Fulton, *Senior Member, IEEE*
and Mark Yeary, *Fellow, IEEE*

***Abstract*—With an incredible increase in the number of wireless devices and an ever-growing demand for high data rates, 5G needs to provide a solution to satisfy demand for the next decade. Multiple-input-multiple-output (MIMO) systems are seen as one of the primary solutions – allowing for spatial multiplexing and the use of millimeter-wave (mmWave) frequencies, which can provide much larger bandwidths and, thus, data rates. MIMO is very closely related to phased arrays, which have been used for radar for the past few decades, and requires many antennas and transceivers – on the order of hundreds or thousands for massive MIMO. To make such systems affordable, low-cost, low-power, and low-complexity is required – inherently compromising other system characteristics, such as linearity. The main focus of this paper will be in summarizing the challenges, recent advances, and potential future breakthroughs concerning MIMO/digital array sensitivity to interferers and nonlinear distortion. Specifically, this paper gives an overview of MIMO/digital array architectures and the different techniques currently researched for the characterization and mitigation of spatial and spectral interferers and nonlinearities, which can be used to extend the effective dynamic range of low-cost MIMO/digital array systems.**

***Index Terms*—MIMO, array signal processing, transceivers, radio spectrum management, nonlinear distortion.**

I. Introduction

THE past decade has seen a great increase in the number of mobile, wireless devices, with data traffic increasing 24-fold from 2010 to 2015, and expected to increase by 500- to 1000-fold from 2010 to 2020 [1], [2]. Smart-devices, such as phones, watches, televisions, and multiple other in-home devices, have created a saturated in-door spectral environment, making up 70 percent of all data consumption [2]. Furthermore, the advent of the Internet-of-Things (IoT), with an estimated 50 billion connected devices by 2020, will increase mobile data traffic to an expected 24 Exabytes per month [3]. Along with this large increase in the number of mobile devices has come a strong demand for increased data rates – due to the desire for high speed mobile internet, smart cars/homes, augmented reality (AR), virtual reality (VR), and IoT [3]. To satisfy this need, data rates are expected to achieve 10-50 Gbps for 5G, compared to the 100 Mbps that 4G provides [3].

This work was partially supported by the Defense Advanced Research Projects Agency (DARPA) under grant no. D15A00090, and by the NOAA Office of Oceanic and Atmospheric Research under NOAA-University of Oklahoma Cooperative Agreement NA11OAR4320072, U.S. Department of Commerce.

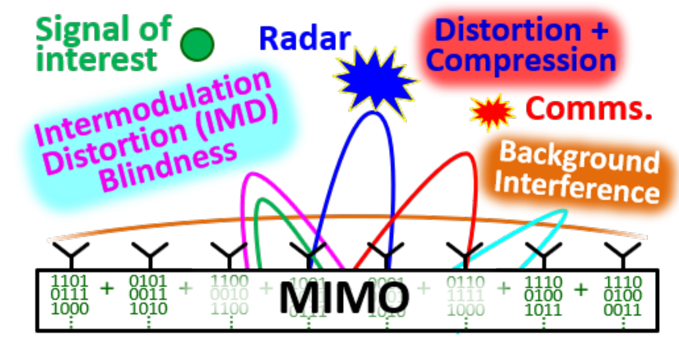

Fig. 1. General MIMO system dealing with multiple interferers and spurs – potentially distorting the signal of interest (SoI) (seen where the purple intermodulation distortion (IMD) is stronger than the green SoI). The IMD caused by the interferers or SoI correlate to apparent directions-of-arrival – ultimately requiring a decorrelation of the IMD at the array level to remove "false signals".

The increase and diversity in Radio Access Technologies (RATs) has forced researchers to look for more efficient ways to use the limited available spectrum. Traditionally, the spectrum bands were allocated for specific services, leading to an inefficient use of the RF spectrum, but recent research has suggested a dynamic sharing of the spectrum based on spatio-temporal needs. To facilitate this idea, the US Federal Communications Commission (FCC) has recently made the 3550-3700 MHz band available, along with 600 MHz of the AWS-3 band [4], [5]. The Citizens Broadband Radio Service (CBRS) bands – 3550-3700 MHz – which were previously dedicated to Naval Radar (3550-3650 MHz) and Fixed Satellite Systems (3650-3700 MHz), recently made available for wireless broadband, have received much attention and research [6]–[10]. The authors of [9], [10] studied the coexistence of Naval Radar and mobile communication systems, further focusing on co-channel and adjacent channel interference. The authors in [7] further studied spectrum sharing in the 5 GHz Unlicensed National Information Infrastructure band, commonly used for WiFi. Additionally, [11] studied the effect of spatio-spectral interference in an unlicensed mmWave band, such as the 60 GHz band. Furthermore, one of the most popular proposed methods for better utilizing the spectrum is through spatial multiplexing.

Multiple-input-multiple-output (MIMO) systems offer a solution to the demands of 5G mobile networks through the use of spatial multiplexing. MIMO systems are related to phased array technology, which has been used for military radar and researched for decades [12]–[15]. MIMO consists of multiple antenna elements for both transmit and receive, improving throughput, capacity, and coverage [16]. MIMO has seen initial uses in some 4G Long-Term Evolution (LTE) standards, wireless local-area-networks (WLAN, IEEE 802.11n, IEEE 802.11ac) [17]–[19], Worldwide Interoperability for Microwave Access (WiMAX) [19], [20], and radar [21]. Massive MIMO, which consists of orders of magnitude more antennas than standard MIMO, will further increase network capacity, and spectral and energy efficiency [14], [16], [22]–[24].

Massive MIMO consists of hundreds of antennas, relying on spatial multiplexing to serve tens of users and increase spectral efficiency [15], [23]. In order to make massive MIMO systems affordable, the elements need to consist of low-cost, low-power, low-complexity components. Creating such systems is one of the major goals for 5G, due to the need for higher network densification and the socioeconomic consequences of expensive systems [2], [14], [23]. Higher network density is required for multiple reasons; higher frequencies – which offer larger bandwidths, and thus, higher data rates, such as millimeter-wave (mmWave) – suffer much more from indirect path loss and therefore have limited non-line-of-sight (NLOS) communication performance. Denser networks also help to reduce power consumption because each base station (BS) will have a shorter radius to cover before another BS takes over coverage. Power requirements can further be reduced in massive MIMO systems because equivalent isotropic radiated power (EIRP) increases by M^2 when the number of antenna elements is increased by M, further reducing both component and operational costs [14].

mmWave, which covers the frequencies of 30-300 GHz, provides a promising solution for the high data rates and spatial flexibility demanded by 5G MIMO systems [11], [25]. The small wavelength of mmWave frequencies will allow MIMO antennas to effectively fit into mobile devices, such as smartphones and IoT sensors, allowing them to take advantage of larger bandwidths and spatial multiplexing. Furthermore, the misconception that higher frequencies suffer insurmountable propagation loss can be invalidated when arrays are used to compensate for loss of physical aperture area [15], [26]–[28]. Therefore, increased propagation loss for line-of-sight (LOS) communications at mmWave frequencies is readily compensated for through the use of multiple antennas. It is important to note that mmWave NLOS communications suffer greater degradation from blocking by obstacles (e.g. buildings, cars, and people) or attenuation from environmental factors (e.g. foliage, precipitation, etc.) relative to traditional "beachfront" frequencies below 6 GHz [26]–[29]. However, such degradation can be compensated for by the additional spatial diversity available at the higher frequencies for sufficiently dense networks [26]. Further, if networks are sufficiently dense, restricted NLOS communications can improve spectral efficiency by using spatial blocking/attenuation to enable spectral re-use by nearby cells. mmWave frequencies have seen initial uses for communication systems in IEEE 802.11ad, which makes use of the unlicensed 60 GHz band [24], [29], [30]. In addition to the 60 Ghz band, the 28-30 GHz, 38 GHz, and 73 GHz bands have also been heavily studied for mobile communications [1], [24]–[26], [29], [31]–[38]. Lastly, mmWave MIMO systems are physically very small, containing many components, and are thus constrained by the need for heat dissipation [34].

One of the most important benefits provided by massive MIMO is the reduction of spatial interference through the use of beamforming, allowing spectrum to be reused for simultaneous communication with multiple users [14]. Using narrow beams can help to mitigate spatial interference, but on the other hand, it increases the risk of link failure [2] – especially in the case of moving users [29], [39]. Furthermore, narrow beams on transmit help add a physical layer of security, preventing eavesdroppers outside of the spatial-beam from detecting the transmission [22]. While narrow beamforming techniques on transmit help to mitigate interfering with other BSs and users, on receive some low-cost massive MIMO systems, like digital phased arrays, are particularly sensitive to interference due to some level of reduction in analog spatial filtering [12]–[15], [40]. This will be exacerbated by the simultaneous operation of 5G small cells and legacy macro cells, leading to irregular cell shapes/sizes and producing inter-cell interference [1]. This is also of concern for WLANs operating in unlicensed bands – such as the industrial, scientific and medical (ISM) band, which are deployed with little to no coordination [1].

In a naively deployed, densely populated systems environment such as WLAN and the initial deployment of 5G BSs operating along with legacy cells, interferers will be a limiting factor of system capacity [14]. Strong, unmitigated interferers decrease the signal-to-interferer-plus-noise ratio (SINR), which, for wireless communication systems, decreases the throughput. Additionally, strong interferers can drive the receiver into compression, producing intermodulation distortion (IMD), further distorting the signal-of-interest (SoI), or even saturating the analog-to-digital converter (ADC). Therefore, it is imperative to implement methods – both analog and digital – to mitigate spatial and spectral interferers along with their residual IMD. Lastly, transmitter nonlinearities, which are typically introduced by the power amplifier (PA), need to be mitigated to prevent the spectral pollution of adjacent channels [41].

The main focus of this paper will be in summarizing the challenges, recent advances, and promising future breakthroughs concerning MIMO/digital array sensitivity to interferers and nonlinear distortion. Section II describes different MIMO/array architectures and physical formats, and then summarizes the dynamic range (DR) issues identified in current transceivers and why it is difficult to quantify these short-comings with current metrics. Next, Section III discusses the trend towards low-cost components, the effects these components have on element and system linearity, and how these issues can be resolved with digital signal processing (DSP). Then, Section IV discusses current technologies for spatial mitigation of interferers for MIMO/array systems. Lastly, Section V will summarize the previous discussions and cover some of the promising future work in these areas.

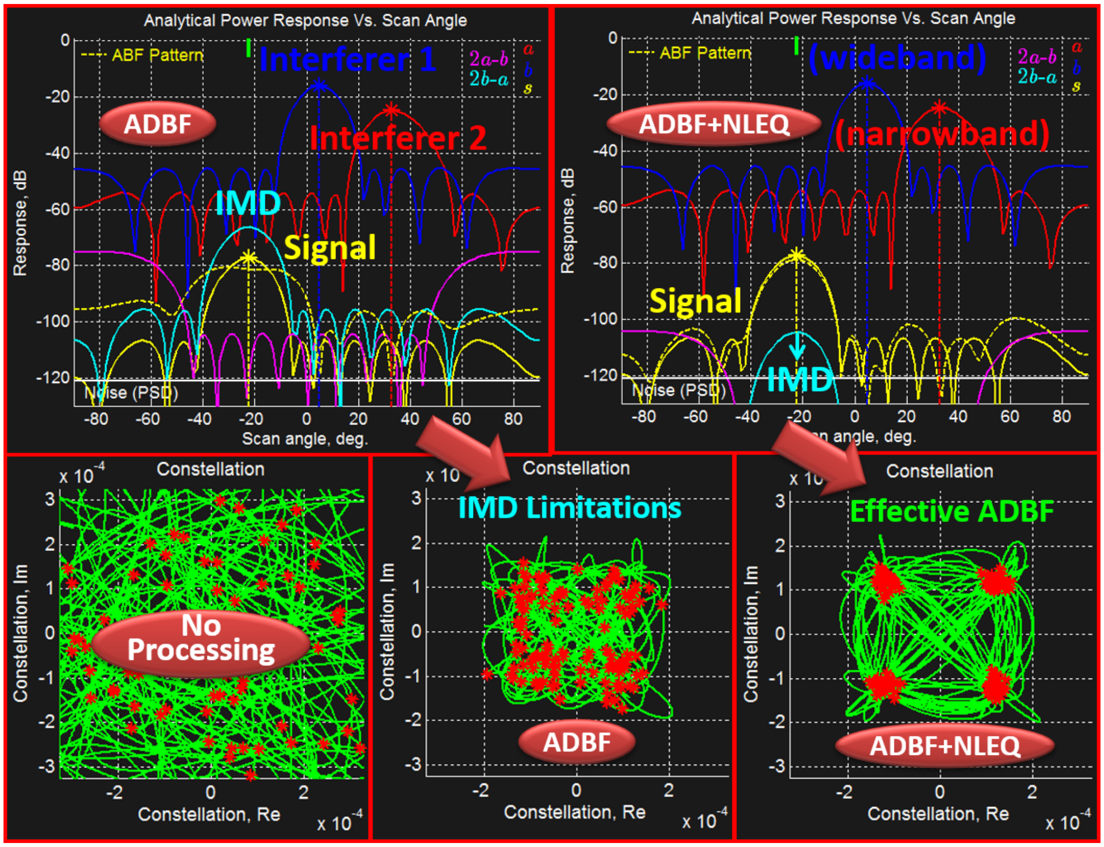

Fig. 2. The team's Matlab Nonlinear Array Simulator (NAS) of element-level distortion and noise based on a 3rd-order, memoryless distortion model. In this case, a strong wideband (blue) and narrowband (red) interferer are keeping a quadrature phase-shift keyed (QPSK) signal at a third angle from being received, confirming that spatial correlation of IMD is predictable and analytically tractable [42]. Even element-level ADBF fails if these IMD products fall in-band and in-angle, even with fairly strong diagonal loading. A simple 3rd-order memoryless NLEQ can help fix this problem, but only if all nonlinearity sources fall within the NLEQ bandwidth.

II. Arrays, Waveforms, Interferers, and Dynamic Range

A. Phased Arrays for 5G/MIMO Applications

Coming from the world of low-cost, highly digital radar, the 5G and massive MIMO visions are extremely intriguing as they seek to leverage the capabilities of phased arrays that the radar community has been refining for the last several decades [12]–[14]. This will not only foster the rapid advancement of phased arrays in general, but possibly enable topics of research that are currently impractical due to excessive initial cost or lack of application space – specifically helped by the increase in access to new commercial off-the-shelf (COTS) components at mmWave frequencies. Phased arrays have laid the groundwork for a huge leap in next-generation networks, enabling spatial multiplexing to allow for efficient reuse of the spectrum.

There are several possible types of phased arrays that should be considered for usage in a 5G network [23]: first is a linear or planar array – these are the most common type of phased arrays and are the most well-understood. When the antenna elements have uniform spacing, these array architectures have many desirable properties such as linear phase progressions during steering, straightforward post-processing algorithms for extracting data, and convenient form factors for manufacturing; this makes them an obvious choice. Furthermore, there are linear and planar arrays with non-uniform element spacing, often referred to as sparse arrays. Due to cost constraints, a non-uniformly spaced array can achieve the same narrow beamwidth of a larger array, without the same number of elements, while also minimizing grating lobes that would otherwise be present in a large array with the same number of uniformly spaced elements and can also lower the sidelobes [43]–[51]. These arrays can be used to reduce cost, while maintaining many of the benefits of uniformly spaced arrays, but can require high computational efforts and increased design complexity. As an alternative to planar arrays, cylindrical arrays are another option.

Several cylindrical testbeds have begun to emerge in recent research [50], [52], [53], showing interest in the problem of a non-planar form factor. Cylindrical arrays have the advantage of higher natural isolation (lower coupling) between polarizations as well as the ability to commute – instead of steer – the pattern around the major axis of the array, resulting in a more consistent pattern, very little to no beam squint, and lower cross-polarization [52], [53]. On the other hand, they do have their share of problems, such as surface waves in the dielectric layers and higher-complexity post-processing to deal with the curve of the array face. Furthermore, sparse cylindrical arrays for massive MIMO were considered in [50], and the mutual coupling of a cylindrical MIMO array of dipoles was studied in [54]. Cylindrical arrays are just the beginning of conformal arrays; dealing with multi-axis curves and different surface materials is an ultimate goal for being able to put arrays on any available surface.

Finally, there are distributed arrays, where elements are spaced many wavelengths apart over a given terrain while still functioning together as a single array. Fig. 1 in [23] provides an excellent visual of this idea; think of many single antennas placed on the top of every building in a metropolitan area. Each antenna is possibly many wavelengths away from its closest neighbor(s), but with a large number of antennas the degrees of freedom can be used to precisely "transmit" to any point in the interior (or even some distance to the exterior) of the enclosed array area. Distributed MIMO systems were studied in [55], demonstrating that distributed antennas achieved higher capacities than co-located antennas for an indoor WiFi-type environment. Furthermore, distributed antenna systems (DAS) can be used in dense urban environments to mitigate the effects of NLOS, where multiple spatially distributed small arrays are deployed to cover certain areas. DAS can be used to reduce power needs as the antennas will be closer to each intended user and to reduce fading loss with the increased likelihood of LOS [39]. The advantages and disadvantages of these array types are being investigated and a clear winner has yet to be identified. As with many engineering problems, the solution is probably to use each type in accordance with their strengths, then find ways to mitigate their weaknesses; though, uniformly spaced planar arrays are the most popular demos and testbeds.

Another important factor in this discussion is the architecture of the transceiver itself. The trend towards low-cost, low-power, highly digital arrays that also have a smaller form factor has decreased the prominence of the superheterodyne transceiver structure, which reigned supreme for the last century of wireless communications [56], [57]. Most handheld devices today employ a homodyne (or direct-conversion) architecture because of the reduced size and complexity (direct conversion receivers do not require image reject filters or multiple intermediate frequency (IF) filters [57], [58]) – and therefore, cost – accompanied by a requisite increase in DSP to maintain performance levels [56], [57]. Though, direct conversion transceivers suffer from many challenges, such as I/Q imbalance, local oscillator (LO) leakage, and both odd and even order nonlinearities [57], [59]–[62]. Another promising architecture is direct sampling, where the analog to digital converter (ADC) is essentially connected directly to the antenna with little to no filtering. This "wide-open" approach seeks to sort through the spectrum digitally, where every process is perfectly linear, easily adaptive, and the primary limitations are maximum input/output power and available processing power.

Additionally, other than the physical layout of the array antennas and the type of transceiver, there are also different amounts of digitization that can be used. Ideally, a fully-digital array would be used to provide maximum flexibility and control over every element. This solution, though optimal, suffers from high cost due to the requirement of N transceivers, and sensitivity to spatial interferers due to the lack of any spatial filtering before the receiver channel [12]–[14], [26], [34], [65]. Hybrid-beamforming methods (sub-arrays) have been studied as a solution to lower cost and add a layer of analog spatial filtering to the arrays, while maintaining the ability to form multiple simultaneous beams [38], [66]–[72]. Sub-arrays are implemented by the combination of multiple small analog arrays, each with N elements per transceiver – where an array with $N{\cdot}M$ total elements will have N elements per sub-array and a total of M transceivers – effectively lowering the transceiver count (cost) by N times [25], [26], [73]. Sub-arrays, on the other hand, suffer from decreased flexibility and multiplexing when compared to fully digital arrays, and introduce grating lobes when the centers of the sub-arrays are separated by more than $\lambda/2$. Overlapped sub-arrays can reduce the transceiver spacing (which directly translates to mitigating or eliminating grating lobes) and are able to efficiently form local beam clusters, but suffer from design and fabrication complexity [12], [25], [65], [74]. Ultimately, low-cost fully-digital arrays offer the most flexibility and highest degree of spatial multiplexing for 5G MIMO systems, but are constrained by their front-end linearity and ability to handle spatial interferers. The later sections of this paper investigate technologies to extend linearity and mitigate spatial interferers.

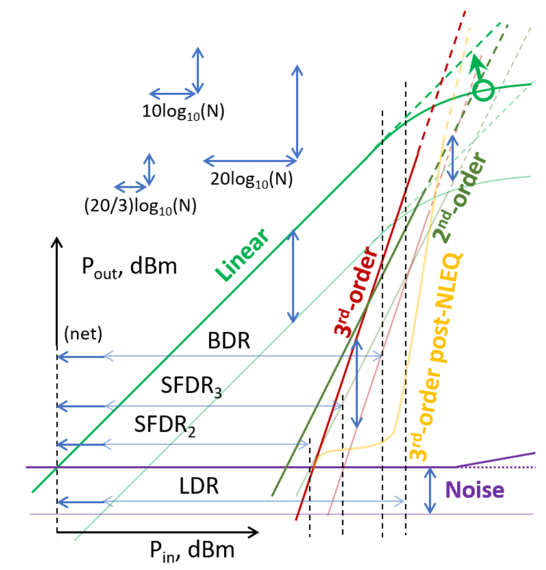

Fig. 3. A summary of the system-level effects of nonlinearity and NLEQ on different types of dynamic range, including the classical Linear Dynamic Range (LDR) [63], second- and third-order Spurious-Free Dynamic Range ($SFDR_2$ and $SFDR_3$ – also using definitions from [63]), and Blocking Dynamic Range (BDR) [64]. The light-colored lines indicate element level values, while the bold lines indicate array level (post-beamforming) values.

This trend towards digitization of transceivers is important because it brings to relevance several of the later topics in this work: the lack of spatial selectivity in the remaining analog front end and the introduction of intermodulation spurs when excess power drives the system into compression; generally this effect happens slowly. When the power-in, power-out curve (like Fig 3) bends gently with increased input power the system is called "weakly" nonlinear. This essentially implies that the nonlinear behavior of the system can be captured with a numerically stable model that has a manageable number of terms [75], [76]. While the transmitter can exhibit this weakly nonlinear behavior (the equalization of power amplifiers (PAs) is known as digital pre-distortion, or DPD), the receiver is especially vulnerable to these effects; "strong" nonlinearities like ADCs can saturate very suddenly, causing model sizes to grow to unmanageable levels or result in numerically unstable coefficients for some terms. This will (sometimes severely) limit the dynamic range of the hardware in such a way that DSP may not be able to recover all or even part of the lost sensitivity. These observations should motivate a deeper discussion of how to quantify and mitigate these emerging problems – using the third-order intercept point and a Taylor series is no longer sufficient to characterize and enhance the high-power behavior of transceiver components [77]. Better metrics will help push research towards the areas that need it, while more complex models will more accurately reflect the behavior of an over-driven system.

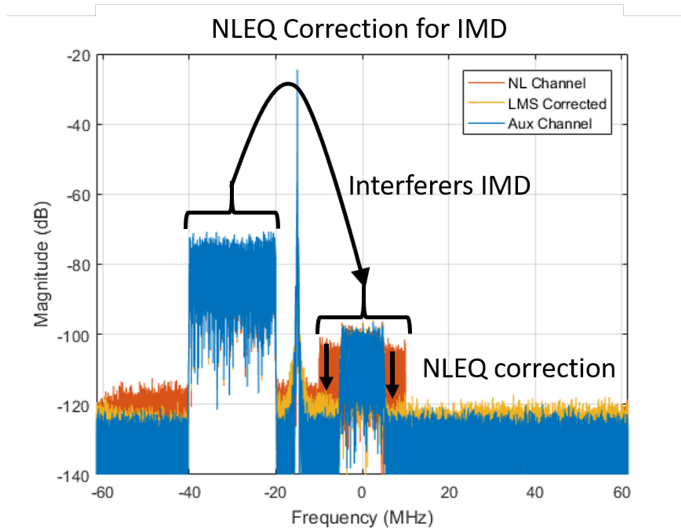

Fig. 4. Example showing IMD from two strong interferers (orange) landing on top of a weak desired signal, which is recovered with an LMS-based NLEQ (yellow).

B. Waveforms

Current LTE communications systems typically use orthogonal frequency division multiplexing (OFDM) waveforms, as seminally discussed in [78]–[80]. In addition to LTE systems, OFDM waveforms have gained popularity within the dual-use radar-communication community, as seen in [81]–[84], and in radar-communications applications, especially for mmWave automotive radar [82], [85]. For communication systems, these links are cyclic prefix (CP-OFDM) for the downlink and the single carrier frequency division multiple access (SC-FDMA) OFDM variant for the uplink [86]–[88]. While the ease of synchronization and orthogonality of CP-OFDM and SC-FDMA have provided high performance to LTE systems, the needs of 5G have caused an ongoing re-examination of communication waveform design and performance [86]–[91]. OFDM signals have large envelope fluctuations due to their high peak-to-average power ratio (PAPR), making them difficult to amplify [92]. In [92] the authors evaluate the capacity, the tight upper bound on the channel data rate, for MIMO-OFDM systems and provides an analytical solution for obtaining the capacity of a given channel. It is shown that the capacity decreases with increased nonlinearity, as expected, but can be compensated by increasing the number of antenna elements.

Moving from LTE to 5G is highlighted by three key needs: the desire for high data-rate ($\sim$10 GB/s) downloads, scalability for the unsynchronized connection of a vast number of low-power devices (i.e. IoT), and a need for ultra-low-latency communications to support the tactile internet [86], [88]. To support these needs many different waveforms have been proposed for 5G with features designed to enable efficient low-latency asynchronous operation and better spectral efficiency, among other goals such as reduced PAPR, robustness to channel selectivity (both temporal and spectral), MIMO compatibility, and computational complexity [86]–[89].

As a starting point, a framework has been proposed for 5G NR Enhanced Mobile Broadband with several key changes over LTE, not the least of which is the targeting of carrier frequencies up to 52.6 GHz [90], [93]. Further standards include extension of bandwidths from 20 MHz to 400 MHz, and of key importance, the asynchronous multiplexing of mixed OFDM numerologies [90], [93]. The wider bandwidths and higher carrier frequencies support the goal for high-speed data rates, while the asynchronous multiplexing of mixed OFDM numerologies enable different providers to occupy adjacent spectral bands and tailor their waveforms to support low-latency communications and/or robustness to increased phase noise from mmWave components [90], [94]. However, it was shown that spectral containment of mixed numerologies was poor, necessitating large guard bands that run counter to the 5G mission of efficient use of spectrum [90]. As such, it was emphasized that the spectrally efficient alternatives with low out-of-band (OOB) emissions developed in the literature would be needed [90].

Unfortunately, while the theoretical properties of these waveforms are well studied, the impact of transmission hardware on spectral efficiency and limiting OOB emissions is only beginning to be considered. Alarmingly, it was shown that the spectral efficiency gains of advanced 5G waveforms (even with low-order modulations) can be completely nullified by spectral regrowth caused by a nonlinear transmit power amplifier [89], [94]. In contrast, it was shown that the OOB emissions of CP-OFDM was largely unaffected as the dominant OOB emissions of CP-OFDM are governed by the $\sin(x)/x$ sidelobes of the rectangular pulse shape.

As a final note on waveforms, the PAPR for the multicarrier waveforms under consideration is still very high [94]. The desire for high order modulations (e.g. 64 or even 256 QAM) further increases the PAPR of any proposed communication waveform and degrades the available transmit power due to transmitter amplifier backoff [91], [95]. While the PAPR of the single carrier waveforms proposed for 5G is lower (particularly for the continuous phase modulated variants), these waveforms are complex and suffer from poor time localization [94]. More pertinent to the focus of this work, the sensitivity of these waveforms due to hardware impairments (i.e. power amplifier nonlinearities and phase noise) has yet to be examined [94].

C. Interferers and Dynamic Range

The classical definition of dynamic range is the ratio between the largest and smallest useful signals at the output of a receiver that is both linear and deterministic [63] – essentially, what the receiver can successfully use for detection. For MIMO communication systems, the dynamic range of each antenna is defined by the strongest blocker and the weakest SoI for all angles, while each beam only sees a dynamic range limited by the blocker and SoI for a particular direction [15]. The main problem is that "largest" and "smallest" are not well-defined terms in a crowded and/or possibly hostile spectrum environment due to the assumption of linearity. In the past, civilian systems were designed in isolation for a specific allocation of spectrum licenses and Tx/Rx only bands, expecting that the system would be allowed to accomplish its mission with little to no interruption from other nearby systems. Modern systems – especially in the communication sector – have outgrown these assumptions. Relaxing the linearity to drive down cost has caused an explosion in the number of active devices in populated areas, effectively ending functional isolation. Because of their new-found pervasiveness, systems can no longer ignore other devices seeking to use the same slice of limited spectrum [5]. Robustness to interference is a major factor in determining the effective DR of a modern digital transceiver, and a system's fitness for use in a MIMO-like network will be largely determined by its ability to reject incoming interference and still serve its intended purpose. Electromagnetic interference (EMI) can skew the effective dynamic range of a transceiver relative to isolated measurements and in some cases can be very difficult to mitigate [60].

Modern digital processing techniques can handle in-band (IB) interference with relative grace when the channels remain linear – adaptive digital beamforming (ADBF) for when there is a separation in the spatial domain [96], and additional digital filtering for when there is separation in the spectral channels. Additionally, if the system is driven some extent into compression so that it is not sufficiently linear anymore, there are nonlinear equalization (NLEQ) techniques summarized in Section III of this work that have been shown to do an excellent job of linearizing the receiver as long as the power does not exceed the maximum training (calibration) levels. A simple example of IMD that lands on a low-power SoI is shown in Fig 4; without some form of NLEQ, this SoI would be unrecoverable for useful data transfer. After effective NLEQ the problem is returned to the previous case of spatial-spectral separation, as shown in Fig 2 where a QPSK signal is distorted by a static third-order polynomial, then extracted using NLEQ and ADBF. Additionally, feed-forward in-band interferer cancellation at baseband was demonstrated in [58] to extend the linearity of the receiver.

OOB blockers can limit receiver linearity and sensitivity, especially in wideband receivers that support a broad tuning range for multi-standard communications with limited front-end RF filtering [98]–[100]. Additionally, OOB interference (OOBI) will become more common as transmitters are forced closer together in the spatial and spectral domains. OOBI scenarios have recently gained interest, having been studied

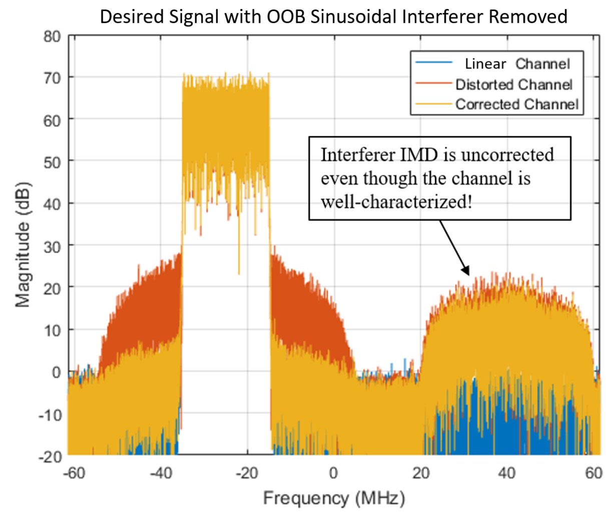

Fig. 5. Example from [97] showing that even with effective IB NLEQ, distortion caused (at least in part) by OOB sources cannot be corrected without some sort of estimation of the magnitude and phase of the OOB signal.

in [98]–[100]. OOBI (here referring to a source that is not only outside the band of operation, but is generally outside the entire digitized bandwidth) is much harder to remove, as the source of interference is not directly observable by the receiver itself. This is clearly demonstrated by the simulation output shown in Fig 5, where a sinusoidal interferer in the roll-off of the channelizing filter has driven the low-noise amplifier (LNA) into compression, resulting in self-distortion on the SoI on the left-hand side and adjacent-channel IMD on the right-hand side of the spectrum. Even after NLEQ – which almost completely removes the self-mixing on the SoI – the adjacent-channel IMD is completely untouched due to the unknown magnitude and phase of the offending sinusoid that gets filtered out before sampling. Thus, the resulting distortion cannot be adequately modeled. There are only a few ways that OOB signals can produce IB distortion: first, one or more close-in (or adjacent-band) signal(s) can mix with an IB signal, causing a form of distortion called "crossmodulation" – this was exhibited in Fig 5. Second, two or more large signals outside the digitized operating bandwidth, but not in a region of high rejection for the analog front end (e.g. adjacent bands, secondary pass bands, etc.), can mix and produce a resultant signal that falls in the band of interest, an example of classic intermodulation. Figure 1 in [4] provides an excellent summary of the taxonomic structure for these types of distortion at third-order. Fundamentally, the issue with OOB interferers is that even though the distortion is directly observable, one or more of the generating signals being fed into the array has an unknown magnitude and phase, making it difficult to model the distortion effectively using digital means. Furthermore, analog and complimentary metal-oxide semiconductor (CMOS) cancellation techniques, while effective, generally add significantly to system complexity. These embedded solutions are discussed in further detail in Section IV. In general, some method of observing the source(s) of the interference is necessary for effective removal. As the spectrum gets more and more crowded, the chances of having a large amount of power (relative to the system's limits) in an inconvenient band continue to rise. Provided that an observation of the interferer can be made, NLEQ techniques can be used to provide mitigation of this type of interferer as well – this is a current topic of research for the authors. But again, this is assuming that the power level is within the training region of available calibrations.

When an interferer pushes the system past its maximum training power level, NLEQ techniques can fail quite suddenly. Without NLEQ, third order spurs increase at a 3:1 rate versus linear signals in the log domain as the power is increased – this is demonstrated in Figure 3 by the light green (linear) and dark red (third-order) traces. NLEQ changes this behavior, mitigating if not eliminating the growth rate of the nonlinear spurs for the trained power range, thus artificially extending the spurious-free [63] and blocking [64] dynamic range (SFDR and BDR, respectively) of the receiver; this suppression effect is shown in light yellow. Once the trained power range is exceeded, however, the growth rate of the spur can *greatly* exceed 3:1 in an effort for the system to return to a "natural" (unequalized) output. This makes measuring the effective dynamic range harder, as it is difficult to predict how the calibration will fail – if it will decay gracefully or become unstable and explode in the digital domain. This further demonstrates the importance of correctly modeling the nonlinear system, both at the channel and array levels.

III. Nonlinear Equalization Technologies

Massive MIMO for 5G wireless networks will make use of low-cost, low-power, low-complexity components in order to properly scale array sizes and provide a high density of base-stations. System-level DR increases linearly with the number of antenna elements, allowing for the use of lower-cost/power/complexity transceivers than are required for legacy systems [13]. Low-cost, low-power RF active components are typically nonlinear in nature [60], [61], [105], causing intermodulation distortion (IMD), harmonic distortion, and compression [106]. Additionally, the characteristics of a nonlinear system can drastically change with power, frequency, and temperature [107]–[111]. A summary of the different types of nonlinear series and polynomials used to model RF nonlinear behavior are included in Table I. These models will be discussed succinctly in the following paragraphs.

The simplest way to represent a nonlinear system is with a static power series polynomial (a Taylor series [101]), often used in digital pre-distortion (DPD). The static power series, though simple, lacks any type of frequency dependence. The Volterra series, on the other hand, provides the most robust and complete polynomial-type representation of nonlinear systems [75], [107], [112], [113], making use of all combinations of power and memory, including numerous cross-terms. While the Volterra series can provide the most precise representation of a nonlinear system, it can contain an enormous number of terms, making it extremely computationally inefficient [76], [107], [113], [114]. There are several simplifications of the Volterra series that improve the computational efficiency and stability of the model at the expense of generality. [103] provides an excellent overview of the different simplifications that can be extracted from the Volterra series; a few of them will be mentioned briefly here – Wiener, Hammerstein, and Memory Polynomial (MP) models.

Wiener models, a special case of the Volterra series, are ones in which the frequency dependence (i.e. memory) comes before a static nonlinearity [102], [103]. In general, this is just the output of an linear time-invariant (LTI) filter being passed into a polynomial. Thus, each "order" being multiplied together already has some sort of frequency dependence to it. As a result, discrete Wiener models are not linear in their coefficients (seen in the coefficients $h[m]$ in Table I) [103], meaning that though the bases of the model are clearly nonlinear, the output is not necessarily a linear combination of the nonlinear bases. This means that the lowest-error set of coefficients is not guaranteed to be found through conventional (read: linear) least-square-error estimation methods. This property makes Wiener systems difficult to handle from a numerical standpoint. Also, the number of coefficients can still be quite large due to the existence of significant cross (mixed-memory) terms, though kernel symmetry can be leveraged to simplify this somewhat.

Hammerstein models, another special case of the Volterra series, on the other hand, have an LTI system *after* the nonlinearity [102], [103]. This is just the linear filtering of a signal that already has some spectral regrowth due to higher-order responses. But, because of this minor rearrangement, discrete Hammerstein models *are* linear in their coefficients, meaning that even though the bases of the model shown in Table I are clearly nonlinear, the coefficients themselves can be obtained using a linear least-square-error approach[1]. This attribute makes Hammerstein models highly preferable to Wiener models when the system can reasonably be assumed to fit the aforementioned parameters – Tx PAs are often modeled as Wiener systems so that the predistorter can be a Hammerstein system (Hammerstein and Wiener models are natural inverses of each other due to model structure), where determining the coefficients is much simpler.

Another common method used to capture a wider array of models is to add more blocks in series with a Wiener or Hammerstein model. A common example of this is the Wiener-Hammerstein model [103], [115], [116]. The Wiener-Hammerstein model is an LTI system followed by a static nonlinearity followed by another LTI system. There are also Hammerstein-Wiener models, which is a static nonlinearity followed by an LTI system and another static nonlinearity [115], [116] – it should be mentioned that this model is much less common than the Wiener-Hammerstein model. But both of these are difficult to use as they exhibit many of the undesirable qualities of the Wiener model while being more complex due to the additional memory or nonlinear element in the system. As an alternate method of adding generality, branches of these models can be added in parallel, adding some flexibility and robustness to the models – resulting in common models such as the parallel Hammerstein (PH) model [102], [113], [117], [118], the parallel Wiener model [103],

[1]This is referenced in [103] in the paragraph immediately following Equation (15); a small amount of rearranging is required to achieve the necessary least-square-error solvable form.

TABLE I
A SUMMARY OF THE DIFFERENT TYPES OF SERIES/POLYNOMIALS TO DESCRIBE COMPLEX BASEBAND NONLINEAR SYSTEMS.

Series Type	Equation
Power Series [101]	$$y(n) = \sum_{p=1}^{P} = a_p x(n)\|x(n)\|^{(p-1)} \quad (1)$$
Volterra Series [102], [103]	$$y(n) = \sum_{p=1}^{P} \left(\sum_{m_1=0}^{M-1} \cdots \sum_{m_p=0}^{M-1} h_p(m_1, ..., m_p) x(k - m_q) \times \prod_{q=1}^{p} \|x(k - m_q)\|^{(q-1)} \right) \quad (2)$$
Wiener Model [102], [103]	$$y(n) = \sum_{p=1}^{P} a_p \left[\sum_{m=0}^{M-1} h(m)x(n-m) \times \left\| \sum_{m=0}^{M-1} h(m)x(n-m) \right\|^{(p-1)} \right] \quad (3)$$
Hammerstein Model [102], [103]	$$y(n) = \sum_{m=0}^{M-1} g(m) \sum_{p=1}^{P} a_p x(n-m)\|x(n-m)\|^{(p-1)} \quad (4)$$
Wiener-Hammerstein Model [103]	$$y(n) = \sum_{m_2=0}^{M-1} g(m_2) \sum_{p=1}^{P} a_p \left[\sum_{m_1=0}^{M-1} h(m_1)x(n - m_1 - m_2) \times \left\| \sum_{m_1=0}^{M-1} h(m_1)x(n - m_1 - m_2) \right\|^{(p-1)} \right] \quad (5)$$
Memory Polynomial [103]	$$y(n) = \sum_{m=0}^{M-1} \sum_{p=1}^{P} a_{mp} x(n-m)\|x(n-m)\|^{(p-1)} \quad (6)$$
Cross-Memory Polynomial [104]	$$y(n) = \sum_{m=0}^{M-1} \sum_{p=1}^{P} a_{pm} x(n-m)\|x(n)\|^{(p-1)} \quad (7)$$
Generalized Memory Polynomial [103]	$$y(n) = \sum_{k=0}^{K_a-1} \sum_{l=0}^{L_a-1} a_{kl} x(n-l)\|x(n-l)\|^k + \sum_{k=0}^{K_b} \sum_{l=0}^{L_b-1} \sum_{m=1}^{M_b} b_{klm} x(n-l)\|x(n-l-m)\|^k + \sum_{k=0}^{K_c} \sum_{l=0}^{L_c-1} \sum_{m=1}^{M_c} c_{klm} x(n-l)\|x(n-l+m)\|^k \quad (8)$$

[113], [114], [119], and the parallel Wiener-Hammerstein model [116].

Due to the complexities of these nonlinear systems, simplified models that provide comparable performance are highly desirable. Many of the recent models and solutions have extended the work above by providing more advanced, simplified models. For instance, approaches to further minimize the number of coefficients have been studied, such as the dynamic deviation reduction-based Volterra series (DDR) [120], [121]. DDR is popular, as it allows for high-order dynamics to be removed from the model, since the effects of dynamics tend to fade with increasing nonlinearity order in many real power amplifiers. Others have relied on the sparsity assumption for the kernel coefficients of the full Volterra behavioral model and combined a greedy algorithm for the selection of the active coefficients [122]. Additional methods specifically devoted to pruning have also been explored. For example, Chen et al., have proposed an error variation ranking (EVR)-based pruning method to reduce the complexity of MPs for power amplifier behavioral modeling in [123]. The authors in [124] have shown some useful convergence properties by expressing the Volterra series as a set of orthogonal functions, when used with a white Gaussian noise input signal. In [125], the authors have employed principal component analysis (PCA) to obtain a reduced order DPD basis that is used to update the DPD coefficients according to a conventional LS formulation. In addition, further complexity reduction was achieved by forcing to zero the less significant terms of the matrix that are used to create the new basis [125]. Finally, [126] developed a "differential-memory" pruning strategy for Volterra series models to further reduce the number of mixed-memory cross-terms in a more algorithmic fashion by limiting the memory spread allowed between distinct signal contributions to a single term of the model.

Finally, MPs provide a good middle ground between computational efficiency and mathematical robustness; they are actually a generalization of the Hammerstein model, and are identical to the parallel Hammerstein model when the nonlinear block is a static polynomial [103], [107], [113]. The MP makes use of M memory terms and P power terms, resulting in $M \cdot P$ total terms that describe both power and frequency dependence of a nonlinear system. The downside is that the MP model lacks any cross-terms (i.e. samples that are multiplied with other samples from a different instant in time), so there is a cross-memory polynomial (CMP) model to include some of these terms when necessary [104]. Lastly, a generalized memory polynomial (GMP) [103] can make be seen as a model that includes a refined number of terms from the Volterra series, thus occupying much of the continuum between the Volterra and MP models.

The previously mentioned mathematical models have been used to characterize and linearize RF components and systems. Both the Tx and Rx have nonlinear components, meaning that both of them suffer from spectral regrowth. Furthermore, there exist multiple different well-researched NLEQ methods for both Tx and Rx nonlinear systems. The following subsections will review the different researched methods for NLEQ, comparing them and discussing the advantages and disadvantages of each model. Lastly, the memory effects present in nonlinear systems should not be ignored, especially for high bandwidth signals [103], [113], [114], [127]–[131].

A. Transmit Nonlinearities

Transmitter nonlinearities and digital pre-distortion (DPD) methods (used to mitigate Tx nonlinearities) have been heavily studied for almost three decades. A simple method to reduce system cost and power consumption is to operate the Tx power amplifier (PA) in the more efficient nonlinear region. Operating in the nonlinear region of a PA creates spurious products caused by IMD; degrading the error vector magnitude (EVM) of the in-band signal and polluting the already saturated wireless spectrum (OOB spectral regrowth is typically measured by the adjacent channel power ratio (ACPR) [128]) shown in Fig. 6 in orange – negatively effecting users in adjacent channels [19], [105], [126], [132], [133]. An efficient method for computing the location (in frequency) and magnitudes of IMD in a transmit PA was presented in [134]. Due to the efficiency benefits of operating in the nonlinear region, DPD has been heavily studied to mitigate the spectral spreading, while retaining the other desirable traits. DPD methods have also been proposed to mitigate Tx I/Q imbalances and crosstalk/mutual coupling present in MIMO systems [19], [59]. This section gives an overview of some of the different DPD techniques in published literature.

A MP model was proposed in [110] to correct power and frequency dependence in a wideband radar amplifier – specifically for use in a digital phased array. The authors also propose a Bayesian method making use of Gibbs sampling, a form of the Markov chain Monte-Carlo (MCMC) algorithm, which – compared to least-squares optimization – is able to gracefully adapt to changes in the amplifier's characteristics, including temperature variations. [135] analyzed the nonlinear distortion in MIMO transmitters caused by PAs. They simulated a 28 GHz, 64-element array with a four-stage class AB GaN MMIC PA, modeled by a memoryless power series. They further show that as the beam is steered and the active impedance of the array changes, then the PA load impedance also changes, degrading the effectiveness of DPD, which was trained at 50 ohms. The authors of [136] developed an impedance-dependent memory polynomial (IDMP) model for DPD of a wideband phased array radar. The IDMP takes into account the dependence on power, frequency, and impedance, all of which are affected by the scan angle and mutual coupling of the array. The IDMP was shown to be more effective than an MP at linearizing the PA of the phased array radar, and was proposed as a potential solution for MIMO communications DPD.

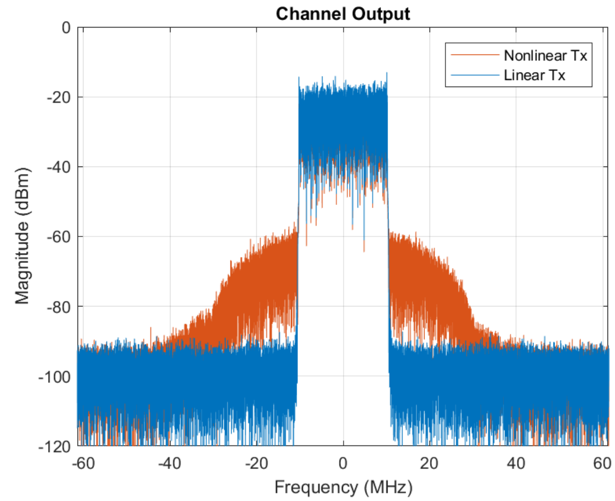

Fig. 6. Nonlinear Tx channel, demonstrating IMD pollution of adjacent channels.

The authors in [137] presented an adaptive DPD method that can be implemented in a field programmable gate array (FPGA) for real-time adaptation. The DPD is made up of a predictive nonlinear auto-regressive moving average (NARMA) that is implemented by means of look-up tables (LUTs). An adaptive least mean-square (LMS) based correction called "nonlinear filtered-x LMS algorithm" with a Volterra series basis was implemented in [138]. The difference for an iterative pre-distortion and post-distortion solution is that the output of the pre-distortion adaptive filter can suffer from instability due to the filter delays. Filtered-x LMS provides an adaptive solutions without causing instability. Additionally, [139] provides a detailed explanation of the LMS algorithm.

A weighted MP (WMP) was proposed in [140] as the basis for the modeling and DPD of a PA. The WMP, given by

$$\begin{aligned} y_{WMP}(n) &= \sum_{i=0}^{N_s} \alpha_i w_s(\mid x(n) \mid) x(n) \mid x(n) \mid^i \\ &+ \sum_{i=1}^{N_D} \sum_{j=1}^{M} \beta_{ij} w_D(\mid x(n) \mid) x(n-j) \mid x(n-j) \mid^i, \end{aligned} \tag{9}$$

is shown to require half as many coefficients as the standard MP to achieve the same performance and is used to better handle high PAPR waveforms which, for a PA, exhibit mild nonlinear behavior and strong memory effects at low power levels, and strong nonlinear behavior with mild memory effects at higher power levels. A finite impulse response (FIR) MP DPD for wideband PAs was proposed in [141]. They showed that the derivation of a MP from the Volterra series is a consequence of the narrowband approximation, which is not valid for wideband signals. Therefore they precede the MP with an FIR filter to further reduce the frequency dependence of the PA. They show that their proposed FIR-MP DPD method further linearizes the PA with an 80 MHz waveform at 2 GHz by providing 11 dB more ACLR improvement. In [104], an FPGA-based DPD solution for PA linearization using a CMP model was provided. They further compare the effectiveness of the CMP model with a MP model with the same number of coefficients. The coefficients are solved for using recursive least squares (RLS), and the CMP proves to perform very similarly to the MP model, both of which greatly outperform the memoryless static power series. They further suggest that their method be implemented in an FPGA for cost-effective nonlinear circuit characterization and modeling. [126] proposed two methods for reducing the complexity of Volterra series, while providing a more robust DPD basis than a simple MP. Methods of grouped Volterra series and pruned Volterra series are discussed and demonstrated for OFDM signals for massive MIMO systems, reducing the ACLR by 4 dB more than a memory-less correction, but showing little improvement over a MP basis. Lastly, the author of [126] states that there is less importance placed on the basis set used for DPD ACLR minimization, as long as the bases themselves span enough effective delays.

The mitigation of PA and I/Q nonidealities was demonstrated in [59]. The authors employed a PH based model, estimating the coefficients using a least squares based technique, showing effective mitigation of IMD for a wideband OFDM signal. MIMO systems also suffer from crosstalk or mutual coupling – which can be nonlinear (before the PA) or linear (at the antenna) [19], [62], [132]. Nonlinear crosstalk can have a great effect on DPD, and the authors of [19] proposed a crossover DPD (CO-DPD) model to mitigate the effects of crosstalk on PA linearization. They showed that CO-DPD could mitigate IMD of the PA almost 30 dB more than conventional DPD when the channel suffered from -20 dB of nonlinear crosstalk. The authors of [132] expanded the crossover model to include the correction of I/Q imbalance. Their measured results showed that their proposed method of the joint mitigation of nonlinearities, I/Q imbalance, and crosstalk resulted in a further reduction of the ACLR by 9 dBc, compared to the crossover model. The joint mitigation of nonlinearities, I/Q imbalance, and crosstalk was further explored in [142], where the authors used a real-valued MIMO MP (RMP) model, which considers the I/Q as separate input signals. This model showed good computational efficiency and effective ACLR mitigation. Additionally, a neural network DPD solution for crosstalk, I/Q imbalance, DC-offset, and PA nonlinearity was presented in [62].

Additionally, DPD has recently been studied for MIMO hybrid beamforming cases, where each digital channel (and its' DPD) should support multiple PAs [105], [143]–[146]. That is, compared to single channel, element-level DPD, hybrid-beamforming DPD requires a single DPD solution for multiple PAs. Furthermore, the PAs in the analog beamformer can each receive different weights, leading to the PAs possibly operating in different nonlinear regions. Beam-oriented DPD was studied in [105], [143], [146] – focusing on the mitigation of IMD in the direction of the main beam and reducing DPD complexity by using one precoder per subarray. Finally, the nonlinear characteristics of each PA in an array differ from one-another and affect using the same DPD for multiple PAs, which was studied in [105], [146], [147].

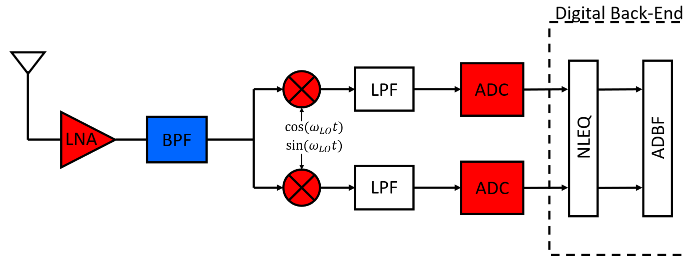

Fig. 7. General nonlinear Rx channel of digital MIMO array with typical nonlinear components in red and the bandpass filter in blue, since it can be linear when active components are used for tuning.

The importance of DPD, especially for low-cost MIMO communication systems, cannot be overstated. DPD allows the PA to operate in the nonlinear region on Tx, which is more power efficient and further lowers the cost of the system. Additionally, DPD helps to lower the ACLR, contributing to a more efficient use of the spectrum and preventing the transmission of energy into sensitive bands – such as global positioning system (GPS) and aviation radar. Further, the most effective DPD methods are ones than can easily adapt to different waveforms and to changes in the nonlinear characteristics of the system due to temperature and/or frequency variations. Lastly, it is worth noting that in 2017 the first RF transceiver with DPD on-chip was released by Analog Devices – the AD9375 [148] – to be used in pre-5G massive MIMO systems. This COTS DPD transceiver is just the beginning of what will enable low-cost 5G systems.

B. Receive Nonlinearities

There are two main differences between DPD and receive-NLEQ. On receive, compared to transmit, there is no *a priori* knowledge of the signals – especially in the case of wireless communications – and signals from multiple sources can move through the channel [149]. Secondly, a receiver chain typically contains a bandpass filter to remove OOB interferers, inducing frequency dependence on the received signals that is unnecessary on the transmit side [111]. Additionally, one of the major concerns of receiver nonlinearities for communications systems is that IMD can fall on top of weak desired signals, distorting the signal and increasing the bit-error-rate (BER) [150]. Lastly, a comprehensive review of analog techniques for linearization of RF receivers is given in [151], while here we continue to focus on DSP-based solutions.

Fig 7 shows a general MIMO array Rx channel consisting of multiple nonlinear components [152]. Perhaps the most studied culprit of Rx channel nonlinearities is the low-noise amplifier

(LNA), due to the low-cost nature of operating in the nonlinear region. This is typically the first component after the antenna, defining the noise figure (NF) of the channel. The LNA is usually followed by a bandpass filter (BPF), used to filter any OOB interferers and the even-order IMD products. The BPF can be either a linear or nonlinear component depending on if it is passive or active, respectively. In reconfigureable systems, which make use of tunable components, the BPF tends to be nonlinear, further contributing to the RF nonlinearities of the system [111]. Additionally, the filter (either passive or active) contributes heavily to the frequency dependence of the channel, requiring the use of memory terms in the NLEQ solution. The in-phase (I) and quadrature (Q) mixers are inherently nonlinear in nature, contributing baseband IMD to the system. Finally, the analog-to-digital converters (ADCs) can also be nonlinear in nature. The nonlinearities of each of these components compound to further increase the complexity of the NLEQ solution. Additionally, it was shown in [42] that IMD spurs in array beams are formed at predictable "apparent" directions, which has also been studied in [60] and [32].

The effect of amplifier nonlinearities on SNR and capacity for wireless communication receivers was studied in [106], showing that the IMD limits the maximum SNR and capacity. An analysis for system receiver nonlinearities in multi-band OFDM (MB-OFDM) systems is proposed in [153], specifically for the first band group of the Multi-Band OFDM Alliance (MBOA) standard [154], which contains three bands of 528 MHz each, in the frequencies between 3.1 and 4.8 GHz. With a maximum power spectral density (PSD) of -41.3 dBm/MHz, this band is particularly sensitive to strong interferers. The authors proposed a technique for the characterization of ultra wide-band (UWB) nonlinear systems, showing that the common two-tone text is only valid for narrow-band (NB) systems. Their proposed technique consists of analyzing the two-tone performance of the entire band, providing simulations to show its effectiveness.

The effect of LNA nonlinearities with memory for wideband spectrum sensing was studied in [155], where the spectral regrowth caused by a low-cost LNA can fall in unused channels, making them appear to have a user. Furthermore, the impact of receiver nonlinearities on spectrum sensing is studied in [152]. They consider the nonlinearities caused by the LNA and mixer, concluding that while the nonlinear distortion of both devices degrade the system performance, the LNA typically dominates the system nonlinearities. LNA and mixer induced receiver nonlinearities was further studied in [149], where the authors demonstrated the modeling and mitigation of RF and BB nonlinearities in direct conversion receivers, such as the receiver in Fig 7. This is accomplished with the use of three adaptive filters (AFs): one for I/Q balance, one for RF nonlinearities, and one for BB nonlinearities – further split into one for each I and Q. Normalized LMS (NLMS), which provides a more stable convergence than standard LMS, was employed along with a memoryless basis. The AFs proved effective at mitigating RF and BB nonlinearities, first for a two-tone input and then with a binary phase-shift keyed (BPSK) input to demonstrate its effectiveness at correcting high-PAPR signals. Lastly, they state that with the use of NLEQ allows for low-cost, low-complexity receiver architectures, specifically in the case of software defined radio (SDR) and cognitive radio (CR). The same authors, in [150], studied the improvement of the BER in Global System for Mobile Communications (GSM) by applying NLEQ. A similar technique was implemented in [156] to mitigate the spectral spreading of a strong BPSK signal that fell on a weak GSM signal. LMS was implemented, along with a real memoryless basis, on an FPGA in an SDR receiver, demonstrating an algorithm and implementation for real-world scenarios. Furthermore, the FPGA implementation proved to make a very efficient use of the computational resources with little processing delay. NLMS was again applied in [41] to implement a blind correction of nonlinearities in a wideband receiver.

An NLEQ method for assisting a tunable channel select filter (CSF) realized in 65 nm CMOS was implemented in [108]. A low-resolution, oversampling auxiliary ADC was used to capture in-band and OOB interferers and IMD, and then applied LMS to mitigate the nonlinearities. The LMS NLEQ did not update continuously to save power, but updated periodically to account for process, voltage, and temperature (PVT) variations. An auxiliary ADC in CMOS was also used in [109] to mitigate nonlinearities and extend the SFDR, specifically for phased array radars. Furthermore, the sampling speed of the auxiliary ADC was reduced to further save power and continual background calibration was used to account for PVT variations, specifically temperature. Lastly, the effectiveness of background calibration compared to single temperature calibration was shown for 10° C to 80° C.

RF NLEQ for direct conversion receivers was further studied in [60], showing that the IMD spurs in a digital array radar (DAR) – in this case consisting of a direct conversion 4x4 digital array and low-cost commercial off-the-shelf (COTS) components – tend to correlate spatially. The RF spurs were mitigated with the use of NLEQ and LO out-phasing. LO outphasing suppresses the even-order spurs through decorrelation – all even order products will have a random phase applied to them so that when DBF is performed, they add in power instead of voltage, giving a $10\log_{10}(N)$ mitigation where N is the number of elements in the array. A weighted least-squares (WLS) version of NLEQ was used to deal with the odd order spurs, which tend to correlate spatially as explained in [42].

Similarly, IMD effects on phased arrays due to interferers was studied in [32]. The authors show the results of the impact of three interferers on a 32-element 28 GHz array for 5G applications by showing how system-level IIP3 changes with scan angle due to the spatial IMD caused by the interferers. This further shows the need for receiver side NLEQ in interferer-filled 5G environments, as well as more effective linearity metrics.

All the previously mentioned methods of NLEQ are applied after the received signal has passed through the RF front-end, meaning that if the incoming signals are too strong they can push the LNA too far into compression for NLEQ to effectively model; at this point the linear signal cannot be completely recovered. Another possibility is for the ADC to saturate, clipping the high-power portions of the signal, which again leads to information loss. This leads to the DR being defined not by the linearity of the RF front-end (when effective NLEQ techniques are implemented), but by its ability to handle strong interferers. To this end, extending the DR of MIMO receivers further requires analog interferer mitigation. Specifically, mitigating strong spatial interferers will suppress the in-band interferers that the RF filter cannot, and will allow the LNA to safely be placed directly after the antenna (before the filter) to minimize the system's NF.

Receiver NLEQ provides a very effective method of mitigating IMD, extending the DR and linearity of low-cost MIMO systems. With the very saturated spectral environment and the lack of inherent spatial filtering in fully-digital arrays and MIMO systems, mitigating nonlinearities caused by strong blocker signals is necessary for operating at the data rates demanded by 5G. Furthermore, adaptive NLEQ solutions that can adjust to different combinations of received signals and to changes in the nonlinear characteristics of the receiver are the most promising for extending the DR and capacity of real 5G MIMO systems.

C. Summary of NLEQ Techniques

In general, a system-specific NLEQ basis such as the pruned Volterra series presented in [126] provides the best combination of computational efficiency (number of computed terms) while remaining a mathematically robust model. Furthermore, it has been shown that an adaptive solution, such as LMS, provides the most dynamic method for mitigation of spectral pollution for Tx and spectral regrowth due to strong interferers for Rx. Lastly, it should be noted that IMD correlate in space (during beamforming), meaning that a two-fold solution is required in mitigating IMD in the individual channels, while also decorrelating the IMD at the array-level. This is of particular importance for the receivers, where IMD, both spatial and spectral, can distort the SoI – especially in the case of strong spatial interferers.

IV. Spatial Interferer Mitigation Techniques

Spatial interferers, which cannot be suppressed with an RF filter, need to be mitigated before the RF front-end lest they distort the SoI. Since early stage removal of interference is highly beneficial, it might seem obvious that the most desirable stage to eliminate the interferer would be at the antenna itself. Antennas have been studied that can be reconfigured in frequency, radiation pattern, polarization, or combinations of reconfigurations [157]–[159]. Pattern reconfigurable antennas (PRA) have been researched for all sorts of scenarios, such as to avoid noise sources or electronic jamming, to improve security, to save energy, and to better detect the SoI in spectrally cluttered environments [157], [160], [161]. In [160], parasitic excitation of elements with switches enabling the antenna to change the maximum angle of the beam was studied. Specifically, switches were used to change the electrical length of resonating lines with the effect of having a reconfigurable Yagi-Uda antenna. Additionally, the polarization reconfigurability of an annular slot antenna was studied in [162], showing the ability to switch between circular and linear polarization. The same authors, in [163], demonstrated a pattern and frequency reconfigurable three-element Yagi-Uda slot array. The reconfigurable slot array was able to scan from $-30°$ to $30°$

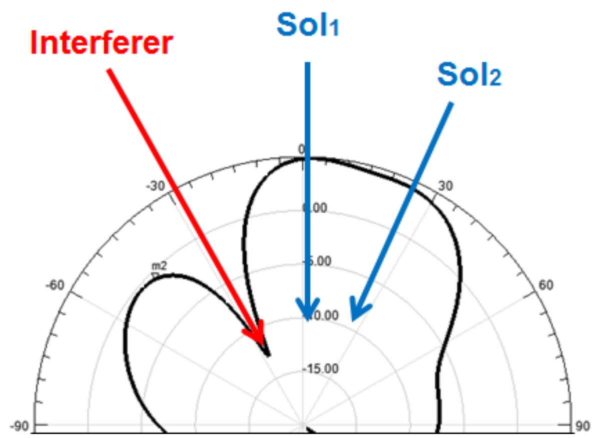

Fig. 8. Illustration of the effect of nulling the embedded element pattern in the direction of the interferer while signals of interest (SoI) are unmitigated

Furthermore, studies have been conducted on the use of PRA for MIMO systems to adapt the radiation pattern of each antenna element in environments with volatile channel conditions [157]. In [157], a reconfigurable U-slot patch with conical and boresight patterns using eight PIN diodes was designed for a 2×2 MIMO-OFDM demonstrator. The PRAs consisted of three states: boresight, symmetrical conical in the z-y plane directed at $44°$, and asymmetrical conical in the z-x plane directed at $45°$. Furthermore, the MIMO-OFDM system consisted of two sets of PRAs, each containing three states, for a total of nine configurations. Using these antennas, system capacity was increased by 17% and 12% for LOS and NLOS, respectively. "Pixelated" PRA's have been explored in [158], [159], [161] where a layer of parasitic pixels connected by PIN diodes is placed above a driven patch antenna. The design in [158] operated in the 2.4 GHz ISM band with nine steerable beam directions and achieved an average of 6 dB of SNR gain compared to legacy omni-directional antennas. A similar design was employed in [161] for the 5 GHz band, which achieved a larger steering range, was able to change the beam width, and had an average gain of 8 dB. The PRA in [159] – also in the 5 GHz band – consists of a single driven dipole enclosed in a 3-D Pin-diode-reconfigurable parasitic layer. This enables the antenna to be steered 360° in azimuth and $\pm 18°$ in elevation – offering a solution to small cell 5G systems. A four subarray PRA was developed in [164], with each subarray consisting of one driven dipole with a parasitic dipole with PIN diodes on either side. The PRA was designed at 5 GHz for handheld devices. Lastly, in [165], PRAs are used to increase the scanning angle of a phased array to $\pm 81°$. The PRA was an annular ring antenna with two parallel slots, fed with strip feedlines containing pin diodes. Additionally, the antenna elements were spaced by greater than half-wavelength, but sidelobes and grating lobes were slightly suppressed with the use of a genetic algorithm. Most of the focus of PRAs has been on beamsteering; however, none of the proposed solutions offer embedded element/antenna pattern steerable nulling which would be optimal for massive MIMO

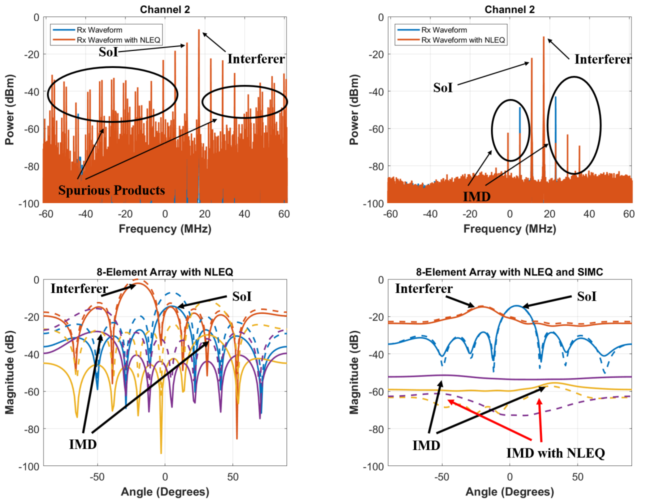

Fig. 9. Example of mitigating a spatial interferer and then applying NLEQ to mitigate channel nonlinearities, ultimately decorrelating the IMD at the array level for a 1x8 digital array. (a) shows the spectrum of channel two with the ADC being saturated by the interferer, with NLEQ (orange) unable to mitigate the IMD. (b) shows the interferer mitigated by the SIMC presented in [40] and the NLEQ further mitigating the IMD. (c) and (d) show the DBF of the array from (a) and (b) respectively.

applications with a dominant, pervasive interference source.

Spatial interference mitigation can also be accomplished by using RF multibeam matrices, such as the Butler matrix [15], [166]. Butler matricies, studied in [167]–[172], are able to provide low-cost spatial selectivity and lack of power consumption since it doesn't use active electronics or processing power. Simultaneous spatio-spectral interference has been demonstrated on CMOS technology using active electronics in RF front-end and baseband [173]–[175]. A 4-element 0.1-1.7 GHz MIMO receiver with spatio-spectral filtering was demonstrated in [173]. The array receiver was designed in 65 nm CMOS, employing a baseband spatial notch filter (SNF) and feed-forward spatial-notch cancellation (FF SNC) to mitigate spatial interferers by 32 dB, with a NF of 2.2-4.6 dB. A 4-element 0.1-3.1 GHz MIMO receiver with analog/RF arbitrary spatial filter was developed in [174]. This receiver improved spatial mitigation to 51-56 dB for a single notch, with a NF of 3.4-5.8 dB. It was also demonstrated that multiple notches could be formed simultaneously. Implementation of spatial interferer mitigation in the CMOS receiver provides a small, scalable solution for digital arrays, but lacks in flexibility as it is not receiver agnostic. RF spatial cancellation achieved by placing a beamformer in the LNA was presented in [176], achieving spatial nulls of more than 20 dB with a NF of 6.7 dB. A different approach using adaptive analog null steering is proposed in [177], where nulls of 20 dB to mitigate the spatial interferer from the grating lobe direction, with a NF of 5 dB, were demonstrated. Lastly, it should be noted that these CMOS receiver architectures have a tradeoff between power and noise figure [178].

Adaptive spatial nulling at the antenna feeding network, before the RF front-end or receiver, was done in [40]. Steerable spatial nulls of more than 20 dB were achieved by interconnecting antenna elements in an array, with the resulting effect of nulling the embedded element pattern as depicted in Fig 8. Direct coupling, through the use of quadrature hybrids, between elements was used to destructively interferen at a certain scan angle. This approach is implemented at the antenna frontend, but, because the SIMC is antenna agnostic, it can be placed at any stage of RF chain and can be used for analog, hybrid, or fully-digital arrays and MIMO systems. Additionally, the measured insertion loss of this circuitry was 1.5 dB; therefore the circuitry could be placed post-LNA for receivers where NF is critical. Finally, Fig. 9 shows the simulated combination of SIMC and NLEQ for a 1x8 digital array. SIMC is used to mitigate the strong spatial interferer, bringing the ADC out of compression. NLEQ is then used to mitigate/decorrelate the IMD, further extending the effective DR of the array.

Omnidirectional antennas have been the antenna of choice for communication systems for decades [30], but arrays and PRAs offer increased capacity and throughput, taking advantage of spatial multiplexing and mitigating multipath effects. Additionally, with low-cost digital and hybrid arrays being sensitive to spatial interferers, analog spatial mitigation capable of high power handling will be necessary to help extend the effective DR and prevent receiver desensitization. The concept in [40] provides a good stepping stone to help deliver the promises of 5G.

V. Conclusion

Massive MIMO, mmWave frequencies, and network densification are the "big three" when it comes to 5G technologies [27]. Two of the limiting factors for future wireless communication networks are linearity and interferer handling of the systems. A review of NLEQ and interferer mitigation techniques for 5G MIMO systems was presented in this paper.

To conclude, system-specific NLEQ bases, such as a pruned Volterra series, provide the best combination of computational efficiency and mathematical robustness. Additionally, adaptive solutions, such as LMS, provide the most dynamic method for mitigation spectral regrowth for both Tx and Rx – being able to adapt to changes in system characteristics due to changes in temperature, frequency, and power. It should also be noted that for arrays, IMD correlate to specific apparent DoAs requiring decorrelation of the IMD at the array-level. Lastly, the Analog Devices AD9375 transceiver is just the beginning of on-chip DPD/NLEQ, which will further enable low-cost 5G systems.

In spatio-spectral crowded environments, with further increases in network densification expected, interferers and blockers are a limiting factor in system performance. This is especially true for element-level digital MIMO systems, which employ little to no spatial filtering. An overview of current research on interferer mitigation techniques for such systems was given in Section IV – with the most effective solution being placed immediately after the antenna, before the interferer is able to drive any active components into compression/saturation. This is an area of research with much to be explored and can provide huge gains in effective system DR for future wireless networks.

REFERENCES

[1] W. H. Chin, Z. Fan, and R. Haines, "Emerging technologies and research challenges for 5G wireless networks," *IEEE Wireless Communications*, April 2014.

[2] P. K. Agyapong, M. Iwamura, D. Staehle, W. Kiess, and A. Benjebbour, "Design considerations for a 5G network architecture," *Proc. IEEE Communications Magazine*, vol. 52, pp. 65–75, November 2014.

[3] M. Benisha, R. T. Prabu, and V. T. Bai, "Requirements and challenges of 5G cellular systems," in *International Conference on Advances in Electrical, Electronics, Information, Communication and Bio-Informatics (AEEICB16)*, 2016.

[4] A. V. Padaki, R. Tandon, and J. H. Reed, "On adjacent channel co-existence with receiver nonlinearity," *IEEE Trans. On Wireless Communications*, vol. 17, pp. 4922–4936, July 2018.

[5] A. V. Padaki, R. Tandon, and J. H. Reed, "Efficient spectrum access and co-existence with receiver nonlinearity: Frameworks and algorithms," *IEEE Trans. On Wireless Communications*, vol. 17, pp. 6404–6418, October 2018.

[6] A. Alsohaily and E. S. Sousa, "The omitted dimension: Exploiting multiuser diversity in multi-radio access technology data cellular communication systems," *IEEE Access*, vol. 4, May 2016.

[7] Y. Ye, D. Wu, Z. Shu, and Y. Qian, "Overview of LTE spectrum sharing technologies," *IEEE Access*, vol. 4, November 2016.

[8] H. Shajaiah, A. Khawar, A. Abdel-Hadi, and T. C. Clancy, "Resource allocation with carrier aggregation in LTE advanced cellular system sharing spectrum with S-band radar," in *2014 IEEE International Symposium on Dynamic Spectrum Access Networks (DYSPAN)*, April 2014.

[9] A. Khawar, A. Abdel-Hadi, and T. C. Clancy, "Spectrum sharing between s-band radar and LTE cellular system: A spatial approach," in *2014 IEEE International Symposium on Dynamic Spectrum Access Networks (DYSPAN)*, April 2014.

[10] N. N. Krishnan, R. Kumbhkar, N. B. Mandayam, I. Seskar, and S. Kompella, "Coexistence of radar and communication systems in CBRS bands through downlink power control," in *2017 IEEE Military Communications Conference (MILCOM) - MILCOM 2017*, October 2017.

[11] S. Niknam, B. Natarajan, and H. Mehrpouyan, "A spatial-spectral interference model for millimeter wave 5G applications," in *2017 IEEE 86th Vehicular Technology Conference (VTC-Fall)*, September 2017.

[12] S. H. Talisa, K. W. O'Haver, T. M. Comberiate, M. D. Sharp, and O. F. Somerlock, "Benefits of digital phased array radar," *Proc. IEEE*, vol. 104, pp. 530–543, March 2016.

[13] C. Fulton, M. Yeary, D. Thompson, J. Lake, and A. Mitchell, "Digital phased arrays: Challenges and opportunities," *Proc. IEEE*, vol. 104, pp. 487–503, March 2016.

[14] A. Puglielli, A. Townley, G. LaCaille, V. Milovanovic, P. Lu, K. Trotskovsky, A. Whitecombr, N. Narevsky, G. Wright, T. Courtade, E. Alon, B. Nikolic, and A. M. Niknejad, "Design of energy- and cost-efficient massive MIMO arrays," *Proc. IEEE*, vol. 104, March 2016.

[15] H. Krishnaswamy and L. Zhang, "Analog and RF interference mitigation for integrated MIMO receiver arrays," *Proc. IEEE*, vol. 104, March 2016.

[16] N. H. M. Adnan, I. M. Rafiqul, and A. Z. Alam, "Massive MIMO for fifth generation (5G): Opportunities and challenges," in *2016 International Conference on Computer & Communication Engineering*, 2016.

[17] *Standard for Information Technology Local and Metropolitan Area Networks Specific Requirements Part 11: Wireless LAN Medium Access Control (MAC) and Physical Layer (PHY) Specifications*. IEEE 802.11n, 2009.

[18] *Standard for Information Technology Telecommunications and Information Exchange between Systems Local and Metropolitan Area Networks Specific Requirements Part 11: Wireless LAN Medium Access Control (MAC) and Physical Layer (PHY) Specifications*. IEEE 802.11ac, 2012.

[19] S. A. Bassam, M. Helaoui, and F. M. Ghannouchi, "Crossover digital predistorter for the compensation of crosstalk and nonlinearity in MIMO transmitters," *IEEE Trans. Microwave Theory and Techniques*, vol. 57, pp. 1119–1128, May 2009.

[20] *Advanced Air Interface, Mobile WiMax*. IEEE 802.16m, 2011.

[21] D. J. Rabideau and P. Parker, "Ubiquitous mimo multifunction digital array radar," in *Thirty-Secenth Asilomar Conference on Signals, Systems & Computers*, November 2003.

[22] E. Yaacoub, M. Husseini, and H. Ghaziri, "An overview of research topics and challenges for 5G massive MIMO antennas," in *2016 IEEE Middle East Conference on Antennas and Propagation (MECAP)*, September 2016.

[23] E. G. Larsson, O. Edfors, F. Tufvesson, and T. L. Marzetta, "Massive MIMO for next generation wireless systems," *Proc. IEEE Communications Magazine*, vol. 52, February 2014.

[24] P. Ferrand, M. Amara, S. Valentin, and M. Guillaud, "Trends and challenges in wireless channel modeling for evolving radio access," *Proc. IEEE Communications Magazine*, vol. 54, pp. 93–99, July 2016.

[25] X. Gao, L. Dai, and A. M. Sayeed, "Low RF-complexity technologies to enable millimeter-wave MIMO with large antenna array for 5G wireless communications," *IEEE Communications Magazine*, April 2018.

[26] W. Roh, J.-Y. Seol, J. Park, B. Lee, J. Lee, Y. Kim, J. Cho, K. Cheun, and F. Aryanfar, "Millimeter-wave beamforming as an enabling technology for 5G cellular communications: Theoretical feasibility and prototype results," *IEEE Communications Magazine*, February 2014.

[27] M. Shafi, A. F. Molisch, P. J. Smith, T. Haustein, P. Zhu, P. D. Silva, F. Tufvesson, A. Benjebbour, and G. Wunder, "5G: A tutorial overview of standards, trials, challenges, deployment, and practice," *IEEE Journal on Selected Areas in Communications*, vol. 35, pp. 1201–1221, June 2017.

[28] N. Bhushan, J. Li, D. Malladi, R. Gilmore, D. Brenner, A. Damnjanovic, R. T. Sukhavasi, C. Patel, and S. Geirhofer, "Network densification: The dominant theme for wireless evolution into 5G," *IEEE Communications Magazine*, vol. 52, pp. 82–89, February 2014.

[29] F. Boccardi, R. W. Heath Jr., A. Lozano, T. L. Marzetta, and P. Popovski, "Five disruptive technology directions for 5G," *IEEE Communications Magazine*, vol. 52, pp. 74–80, February 2014.

[30] C. J. Hansen, "WiGig: Multi-gigabit wireless communications in the 60 GHz band," *IEEE Wireless Communications*, vol. 18, pp. 6–7, December 2011.

[31] F. Al-Ogaili and R. M. Shubair, "Millimeter-wave mobile communications for 5G: Challenges and opportunities," in *IEEE International Symposium on Antennas and Propagation (APSURSI)*, June 2016.

[32] B. Rapakula and G. M. Rebeiz in *Intermodulation Effects and System Sensitivity Degradation in 5G Phased-Arrays due to Multiple Interferers*, June 2018.

[33] S. Kim, Y. Jeon, G. Noh, Y. O. Park, I. Kim, and H. Shin, "A 2.59-GHz RF self-interference cancellation circuit with wide dynamic range for in-band full-duplex radio," *IEEE MTT-S International Microwave Symposium Digest*, vol. 2016-Augus, pp. 4–7, 2016.

[34] B. Yang, Z. Yu, J. Lan, R. Zhang, J. Zhou, and W. Hong, "Digital beamforming-based massive MIMO transceiver for 5G millimeter-wave communications," *IEEE Transactions on Microwave Theory and Techniques*, vol. 66, July 2018.

[35] J. N. Murdock, E. Ben-Dor, Y. Qiao, J. I. Tamir, and T. S. Rappaport, "A 38 GHz cellular outage study for an urban outdoor campus environment," in *IEEE Wireless Communications and Networking Conference (WCNC)*, April 2012.

[36] H. Zhao, R. Mayzus, S. Sun, M. Samimi, J. K. Schulz, Y. Azar, K. Wang, G. N. Wong, J. Felix Gutierrez, and T. S. Rappaport, "28 GHz millimeter wave cellular communication measurements for reflection and penetration loss in and around buildings in New York City," in *IEEE International Conference on Communications (ICC)*, June 2013.

[37] T. S. Rappaport, S. Sun, R. Mayzus, H. Zhao, Y. Azar, K. Wang, G. N. Wong, J. K. Shulz, M. Sammi, and F. Gutierrez, "Millimeter wave mobile communications for 5G cellular: It will work!," *IEEE Access*, vol. 1, May 2013.

[38] S. Mondal, R. Singh, and J. Paramesh, "A reconfigurable 28/37 GHz hybrid-beamforming MIMO receiver with inter-band carrier aggregation and RF-domain LMS weigh adaptation," in *IEEE International Solid-State Circuits Conference (ISSCC)*, February 2018.

[39] J. Zhang, Z. Ge, Q. Li, M. Guizani, and Y. Zhang, "5G millimeter-wave antenna array: Design and challenges," *IEEE Wireless Communications*, vol. 24, April 2017.

[40] R. Irazoqui and C. Fulton, "Spatial interference mitigation nulling the embedded element pattern," in *2018 IEEE/MTT-S International Microwave Symposium (IMS)*, pp. 620–623, June 2018.

[41] R. Vansebrouck, C. Jabbour, P. Desgreys, O. Jamin, and V.-T. Nguyen, "Performance study of nonlinearities blind correction in wideband receivers," in *Proc. 21st IEEE International Conference Electronics, Circuits, and Systems (ICECS)*, December 2014.

[42] C. Hemmi, "Pattern characteristics of harmonic intermodulation products in broadband active transmit arrays," *IEEE Trans. Antennas and Propagation*, vol. 50, pp. 858–865, August 2002.

[43] H. Unz, "Linear arrays with arbitrarily distributed elements," *IRE Trans. Antennas and Propagation*, vol. 8, March 1960.

[44] R. Harrington, "Sidelobe reduction by nonuniform element spacing," *IRE Trans. Antennas and Propagation*, vol. 9, March 1961.

[45] M. G. Andreasen, "Linear arrays with variable interelement spacings," *IRE Trans. Antennas and Propagation*, vol. 10, March 1962.

[46] A. Ishimaru, "Theory of unequally-spaced arrays," *IRE Trans. Antennas and Propagation*, vol. 10, November 1962.

[47] R. M. Leahy and B. D. Jeffs, "On the design of maximally sparse beamforming arrays," *IEEE Trans. Antennas and Propagation*, vol. 39, August 1991.

[48] W. Roberts, L. Xu, J. Li, and P. Stoica, "Sparse antenna array design for MIMO active sensing applications," *IEEE Trans. Antennas and Propagation*, vol. 59, March 2011.

[49] D. Overturf, K. Buchanan, J. Jensen, C. Flores-Molina, S. Wheeland, and G. H. Huff, "Investigation of beamforming patterns from volumetrically distributed phased arrays," in *2017 IEEE Military Communications Conference (MILCOM)*, October 2017.

[50] N. Wu, F. Zhu, and Q. Liang, "Evaluating spatial resolution and channel capacity of sparse cylindrical arrays for massive MIMO," *IEEE Access*, vol. 5, October 2017.

[51] Z. Peng and C. Li, "A portable K-band 3-D MIMO radar with nonuniformly spaced array for short-range localization," *IEEE Trans. Microwave Theory and Techniques*, vol. 66, pp. 5075–5086, November 2018.

[52] G. Zhang, R. J. Doviak, D. S. Zrnic, R. Palmer, L. Lei, and Y. Al-Rashid, "Polarimetric phased-array radar for weather measurement: A planar or cylindrical configuration?," *Journal of Atmospheric and Oceanic Technology*, vol. 28, January 2011.

[53] C. Fulton, G. Zhang, W. Bocangel, L. Lei, R. Kelley, and M. McCord, "Cylindrical polarimetric phased array radar: A multi-function demonstrator and its calibration," in *2013 IEEE International Conference on Microwaves, Communications, Antennas and Electronic Systems (COMCAS 2013)*, October 2013.

[54] B. Cordill, J. Metcalf, S. A. Seguin, D. Chatterjee, and S. D. Blunt, "The impact of mutual coupling on MIMO radar emissions," in *International Conference on Electromagnetics in Advanced Applications*, September 2011.

[55] R. Ibernon-Fernandez, J.-M. Molina-Garcia-Pardo, and L. Juan-Llacer, "Comparison between measurements and simulations of conventional and distributed MIMO system," *IEEE Antennas and Wireless Propagation Letters*, vol. 7, August 2008.

[56] S. Mattisson, "Architecture and technology for multistandard transceivers," in *2001 BIPOLAR/BiCMOS Circuits and Technology Meeting*, October 2001.

[57] A. Loke and F. Ali, "Direct conversion radio for digital mobile phones – design issues, status, and trends," *IEEE Trans. Microwave Theory and Techniques*, vol. 50, pp. 2422–2435, November 2002.

[58] A. Balankutty and P. R. Kinget, "An ultra-low voltage, low-noise, high linearity 900-MHz receiver with digitally calibrated in-band feed-forward interferer cancellation in 65-nm CMOS," *IEEE Journal of Solid-State Circuits*, vol. 46, pp. 2268–2283, October 2011.

[59] L. Anttila, P. Handel, and M. Valkama, "Joint mitigation of power amplifier and I/Q modulator impairments in broadband direct-conversion transmitters," *IEEE Trans. Microwave Theory and Techniques*, vol. 58, pp. 730–739, April 2010.

[60] B. James and C. Fulton, "Decorrelation and mitigation of spurious products in phased arrays with direct conversion transceivers," *Proc. 2015 IEEE MTT-S International Microwave Symposium*, pp. 1–3, May 2015.

[61] M. Abdelaziz, L. Anttila, and M. Valkama, "Reduced-complexity digital predistortion for massive MIMO," in *2017 IEEE International Conference on Acoustics, Speech and Signal Processing (ICASSP)*, March 2017.

[62] P. Jaraut, M. Rawat, and F. M. Ghannouchi, "Composite neural network digital predistortion model for joint mitigation of crosstalk, I/Q imbalance, nonlinearity in MIMO transmitters," *IEEE Trans. Microwave Theory and Techniques*, vol. 66, pp. 5011–5020, November 2018.

[63] D. M. Pozar, *Microwave Engineering*. Hoboken, New Jersey: Wiley, 4th ed., 2012.

[64] V. Gregers-Hansen and M. T. Ngo, "Radar dynamic range specification and measurement," in *Proc. 2009 International Radar Conference*, October 2009.

[65] J. S. Herd and M. D. Conway, "The evolution to modern phased array architectures," *Proc. IEEE*, vol. 104, March 2016.

[66] X. Zhang, A. F. Molisch, and S.-Y. Kung, "Variable-phase-shift-based rf-baseband codesign for MIMO antenna selection," *IEEE Trans. on Signal Processing*, vol. 53, pp. 4091–4103, November 2005.

[67] R. J. Mailloux, S. G. Santarelli, T. M. Roberts, and D. Luu, "Irregular polyomino shaped subarrays for space-based active arrays," *International Journal of Antennas and Propagation*, vol. 2009, 2009.

[68] R. J. Mailloux and S. G. Santarelli, "Mutual coupling effects and their compensation in a time-delay scanned array of irregular subarrays," *IEEE Antennas and Propagation Letters*, vol. 12, pp. 657–660, May 2013.

[69] F. Sohrabi and W. Yu, "Hybrid digital and analog beamforming design for large-scale antenna arrays," *IEEE Journal of Selected Topics in Signal Processing*, vol. 10, pp. 501–513, April 2016.

[70] Z. Li, S. Han, and A. F. Molisch, "Hybrid beamforming design for millimeter-wave multi-user massive MIMO downlink," in *2001 BIPOLAR/BiCMOS Circuits and Technology Meeting*, October 2001.

[71] P. Xingdong, H. Wei, Y. Tianyang, and L. Linsheng, "Design and implementation of an active multibeam antenna system with 64 RF channels and 256 antenna elements for Massive MIMO application in 5G wireless communications," *China Communications*, vol. 11, pp. 16–23, November 2014.

[72] C. T. Neil, A. Garcia-Rodriguez, P. J. Smith, P. A. Dmochowski, C. Masouros, and M. Shafi, "On the performance of spatially correlated large antenna arrays for millimeter-wave frequencies," *IEEE Trans. on Antennas and Propagation*, vol. 66, pp. 132–146, January 2018.

[73] D. R. Fuhrmann, J. P. Browning, and M. Rangaswamy, "Advanced signaling strategies for the hybrid MIMO phased-array radar," in *IEEE Radar Conference*, May 2010.

[74] J. Herd and S. Duffy, "Overlapped digital subarray architecture for multiple beam phased array radar," in *5th European Conference on Antennas and Propagation (EuCAP)*, April 2011.

[75] W. J. Rugh, *Nonlinear System Theory: The Volterra/Wiener Approach*. Baltimore, Maryland: The Johns Hopkins University Press, 1981.

[76] V. J. Mathews and G. L. Sicuranza, *Polynomial Signal Processing*. New York, New York: Wiley, 2000.

[77] A. V. Padaki and J. H. Reed, "Impact of intermodulation distortion on spectrum preclusion for DSA: A new figure of merit," in *2014 IEEE International Symposium on Dynamic Spectrum Access Networks (DYSPAN)*, April 2014.

[78] Y. Wu and W. Y. Zou, "Orthogonal frequency division multiplexing: A multi-carrier modulation scheme," *IEEE Transactions on Consumer Electronics*, vol. 41, pp. 392–399, August 1995.

[79] J. A. Bingham, "Multicarrier modulation for data transmission: An idea whose time has come," *IEEE Communications Magazine*, vol. 28, pp. 5–14, May 1990.

[80] H. Sari, G. Karam, and I. Jeanclaude, "Transmission techniques for digital terrestrial TV broadcasting," *IEEE Communications Magazine*, vol. 33, pp. 100–109, February 1995.

[81] G. Franken, H. Nikookar, and P. van Genderen, "Doppler tolerance of OFDM-coded radar signals," in *2006 European Radar Conference*, September 2006.

[82] C. Sturm, T. Zwick, and W. Wiesbeck, "An OFDM system concept for joint radar and communications operations," in *IEEE 69th Vehicular Technology Conference - VTC Spring 2009*, April 2009.

[83] S. Sen and A. Nehorai, "Target detection in clutter using adaptive OFDM radar," *IEEE Signal Processing Letters*, vol. 16, pp. 592–595, April 2009.

[84] D. Garmatyuk, J. Schuerger, Y. T. Morton, K. Binns, M. Durbin, and J. Kimani, "Feasibility study of a multi-carrier dual-use imaging radar and communication system," in *2007 European Radar Conference*, October 2007.

[85] C. Sturm and W. Wiesbeck, "Waveform design and signal processing aspects for fusion of wireless communications and radar sensing," *Proc. IEEE*, vol. 99, pp. 1236–1259, May 2011.

[86] P. Banelli, S. Buzzi, G. Colavolpe, A. Modenini, F. Rusek, and A. Ugolini, "Modulation formats and waveforms for 5G networks: Who will be the heir of OFDM?: An overview of alternative modulation schemes for improved spectral efficiency," *IEEE Signal Processing Magazine*, vol. 31, pp. 80–93, October 2014.

[87] A. Hammoodi, L. Audah, and M. A. Taher, "Green coexistence for 5G waveform candidates: A review," *IEEE Access*, January 2019.

[88] G. Wunder, P. Jung, M. Kasparick, T. Wild, F. Schaich, Y. Chen, S. T. Brink, I. Gaspar, N. Michailow, A. Festag, L. Mendes, N. Cassiau, D. Ktenas, M. Dryjanski, S. Pietrzyk, B. Eged, P. Vago, and F. Wiedmann, "5GNOW: non-orthogonal, asynchronous waveforms for future mobile applications," *Proc. IEEE Communications Magazine*, vol. 52, pp. 97–105, February 2014.

[89] H. Wang, A. A. Zaidi, X. Chen, J. Luo, and M. Dieudonne, "Evaluation of 5G waveform candidates considering hardware impairments and above 6 GHz operation," in *2017 IEEE 85th Vehicular Technology Conference (VTC-Fall)*, June 2017.

[90] D. Demmer, R. Gerzauet, J. Dore, and D. L. Ruyet, "Analytical study of 5G NR eMBB coexistence," pp. 186–190, June 2018.

[91] T. Levanen, K. Pajukoski, M. Renfors, and M. Valkama, "Cost of increased bandwidth efficiency in 5G NR," in *2017 IEEE 86th Vehicular Technology Conference (VTC-Fall)*, September 2017.

[92] P. Fernandes, J. Guerreiro, R. Dinis, and P. Montezuma, "On the capacity of nonlinear massive MIMO-OFDM systems," in *2016 IEEE 84th Vehicular Technology Conference (VTC-Fall)*, September 2016.

[93] 3rd Generation Partnership Project (3GPP), "Overall description stage 2," *Technical Specification Group Access Network*.

[94] A. A. Zaidi, J. Luo, R. Gerzaguet, H. Wang, X. Chen, Y. Qi, N. Cassiau, A. Wolfgang, J. Vihriala, A. Kakkavas, T. Svensson, J. Mohammadi, R. J. Weiler, M. Dieudonne, H. Halbauer, V. Moles-Cases, and H. Miao, "Evaluation of waveforms for mobile radio communications above 6 GHz," in *Proc. 2016 IEEE Globecom Workshops (GC Wkshps)*, December 2016.

[95] J. G. Proakis and M. Salehi, *Digital Communications*. McGraw-Hill, 2008.

[96] M. A. Richards, *Fundamentals of Radar Signal Processing*, pp. 465–471. New York, New York: McGraw-Hill, 2005.

[97] B. James and C. Fulton, "Nonlinear array system modeler for advanced array calibration," in *Proc. GOMACTech 2017*, March 2017.

[98] P. Sepidband and K. Entesari, "A CMOS wideband receiver resilient to out-of-band blockers using blocker detection and rejection," *IEEE Trans. Microwave Theory and Techniques*, vol. 66, pp. 2340–2355, May 2018.

[99] Y. Zhang, J. Zhu, and P. R. Kinget, "An out-of-band IM3 cancellation technique using a baseband auxiliary path in wideband LNTA-based receivers," *IEEE Trans. Microwave Theory and Techniques*, vol. 66, pp. 2580–2591, June 2018.

[100] A. Rasekh and M. S. Bakhtiar, "Effect of out-of-band blockers on the required linearity, phase noise, and harmonic rejection of SDR receivers without input SAW filter," *IEEE Trans. Microwave Theory and Techniques*, vol. 66, pp. 4913–4926, November 2018.

[101] M. Schetzen, "Nonlinear system modeling based on the Wiener theory," *Proc. IEEE*, vol. 69, pp. 1557–1573, December 2981.

[102] M. Isaksson, D. Wisell, and D. Ronnow, "A comparative analysis of behavioral models for RF power amplifiers," *IEEE Trans. Microwave Theory and Techniques*, vol. 54, pp. 348–359, January 2006.

[103] D. Morgan, Z. Ma, J. Kim, M. Zierdt, and J. Pastalan, "A generalized memory polynomial model for digital predistortion of RF power amplifiers," *IEEE Trans. Signal Processing*, vol. 54, pp. 3852–3860, October 2006.

[104] G. L. Cunha, S. Farsi, B. Nauwelaers, and D. Schreurs, "An FPGA-based digital predistorter for RF power amplifier linearization using cross-memory polynomial model," *International Workshop on Integrated Nonlinear Microwave and Millimeter-wave Circuits (INMMiC)*, pp. 1–3, 2014.

[105] M. Abdelaziz, L. Antilla, A. Brihuega, F. Tufvesson, and M. Valkama, "Digital predistortion for hybrid MIMO transmitters," *IEEE Journal of Selected Topics in Signal Processing*, vol. 12, pp. 445–454, June 2018.

[106] P. Xue, H. Yang, Z. Xu, C. Zhou, and S. Zhou, "Effect of nonlinearities in wireless communication with digital receiver," in *2013 IEEE Wireless Communications and Networking Conference (WCNC)*, April 2013.

[107] A. S. Tehrani, H. Cao, S. Afsardoost, T. Eriksson, M. Isaksson, and C. Fager, "A comparative analysis of the complexity/accuracy tradeoff in power amplifier behavioral models," *IEEE Trans. Microwave Theory and Techniques*, vol. 58, pp. 1510–1520, June 2010.

[108] R. Gangarajaiah, M. Abdulaziz, H. Sjoland, P. Nilsson, and L. Liu, "A digitally assisted nonlinearity mitigation system for tunable channel select filters," *IEEE Trans. Circuits Systems II, Express Briefs*, vol. 63, January 2016.

[109] S. Chen and B. Murmann, "An 8-bit 1.25GS/s CMOS IF-sampling ADC with background calibration for dynamic distortion," in *IEEE Asian Solid-State Circuits Conference (A-SSCC)*, November 2016.

[110] Z. Dunn, M. Yeary, C. Fulton, and N. Goodman, "Wideband digital predistortion of solid-state radar amplifiers," *IEEE Transactions on Aerospace and Electronic Systems*, vol. 52, pp. 2452–2466, October 2016.

[111] N. Peccarelli and C. Fulton, "Adaptive nonlinear equalization of a tunable bandpass filter," *IEEE Microwave and Wireless Components Letters*, vol. 29, pp. 149 – 151, February 2019.

[112] M. Schetzen, *The Volterra and Wiener Theories of Nonlinear Systems*. New York, New York: Wiley, 1st ed., 1980.

[113] L. Ding, G. T. Zhou, D. R. Morgan, Z. Ma, J. S. Kenny, J. Kim, and C. R. Giardina, "A robust digital baseband predistorter constructed using memory polynomials," *IEEE Trans. on Communications*, vol. 52, pp. 159–165, January 2004.

[114] H. Ku, M. D. McKinley, and J. S. Kenny, "Quantifying memory effects in RF power amplifiers," *IEEE Trans. Microwave Theory and Techniques*, vol. 50, pp. 2843–2849, December 2002.

[115] N. J. Bershad, P. Celka, and S. McLaughlin, "Analysis of stochastic gradient identification of Wiener-Hammerstein systems for nonlinearities with hermite polynomial expansions," *IEEE Trans. on Signal Processing*, vol. 49, pp. 1060–1072, May 2001.

[116] M. Schoukens, G. Vandersteen, and Y. Rolain, "An identification algorithm for parallel Wiener-Hammerstein systems," in *52nd IEEE Conference on Decision and Control*, December 2013.

[117] M. Schoukens, Y. Rolain, R. Pintelon, and J. Schoukens, "Semi-parametric identification of parallel Hammerstein systems," in *UKACC International Conference on Control 2010*, September 2010.

[118] M. Schoukens, R. Pintelon, and Y. Rolain, "Parametric identification of parallel Hammerstein systems," *IEEE Transactions on Instrumentation and Measurement*, vol. 60, pp. 3931–3938, December 2011.

[119] M. Schoukens and Y. Rolain, "Parametric identification of parallel Wiener systems," *IEEE Transactions on Instrumentation and Measurement*, vol. 61, pp. 2825–2832, October 2012.

[120] A. Zhu, P. J. Draxler, J. J. Yan, T. J. Brazil, D. F. Kimball, and P. M. Asbeck, "Open-loop digital predistorter for rf power amplifiers using dynamic deviation reduction-based Volterra series," *IEEE Trans. Microwave Theory and Techniques*, vol. 56, pp. 1524–1534, June 2008.

[121] L. Guan and A. Zhu, "Simplified dynamic deviation reduction-based Volterra model for Doherty power amplifiers," *2011 Workshop on Integrated Nonlinear Microwave and Millimeter-wave Circuits (INMMiC)*, April 2011.

[122] J. Reina-Tosina, M. Allegue-Martinez, C. Crespo-Cadenas, C. Yu, and S. Cruces, "Behavioral modeling and predistortion of power amplifiers under sparsity hypothesis," *IEEE Trans. Microwave Theory and Techniques*, vol. 63, pp. 745–753, February 2015.

[123] W. Chen, S. Zhang, Y.-J. Liu, F. M. Ghannouchi, Z. Feng, and Y. Liu, "Efficient pruning technique of memory polynomial models suitable for pa behavioral modeling and digital predistortion," *IEEE Trans. Microwave Theory and Techniques*, vol. 62, pp. 2290–2299, October 2014.

[124] F. Mkadem, D. Y.-T. Wu, and S. Boumaiza, "Wiener G-functionals for nonlinear power amplifier digital presistortion," in *2012 IEEE/MTT-S International Microwave Symposium Digest*, June 2012.

[125] P. L. Gilabert, G. Montoro, D. Lopez, N. Bartzoudis, E. Bertan, M. Payaro, and A. Hourtane, "Order reduction of wideband digital predistorters using principal component analysis," in *2013 IEEE MTT-S International Microwave Symposium Digest*, June 2013.

[126] R. N. Braithwaite, "Digital predistortion of an RF power amplifier using a reduced Volterra series model with a memory polynomial estimator," *IEEE Trans. Microwave Theory and Techniques*, vol. 65, pp. 3613–3623, October 2017.

[127] W. Bosch and G. Gatti, "Measurement and simulation of memory effects in predistortion linearizers," *IEEE Trans. Microwave Theory and Techniques*, vol. 37, pp. 1885–1890, December 1989.

[128] J. F. Sevic, K. L. Burger, and M. B. Steer in *A Novel Envelope-Termination Load-Pull Method for ACPR Optimization of RF/Microwave Power Amplifiers*, June 1998.

[129] J. Lajoinie, E. Ngoya, D. Barataud, J. Nebus, J. Sombrin, and B. Rivierre in *Efficient Simulation of NPR for the Optimum Design of Satellite Transponders SSPAs*, June 1998.

[130] H. Ku and J. S. Kenny, "Behavioral modeling of nonlinear rf power amplifiers considering memory effects," *IEEE Trans. Microwave Theory and Techniques*, vol. 51, pp. 2495–2504, December 2003.

[131] J. C. Pedro and S. A. Maas, "A comparative overview of microwave and wireless power-amplifier behavioral modeling approaches," *IEEE Trans. Microwave Theory and Techniques*, vol. 53, pp. 1150–1163, April 2005.

[132] D. Saffar, N. Boulejfen, F. Ghannouchi, M. M. Helaoui, and A. Gharssalah, "Compensation of I/Q impairments and nonlinear distortion in MIMO wireless transmitters," in *2013 IEEE 11th International New Circuits and Systems Conference (NEWCAS)*, September 2013.

[133] M. Abdelaziz, L. Anttila, A. Kiayani, and M. Valkama, "Decorrelation-based concurrent digital predistortion with a single feedback path," *IEEE Trans. Microwave Theory and Techniques*, vol. 66, pp. 280–293, January 2018.

[134] M. B. Yeary, "An efficient intermodulation product computing technique for broadband active transmit systems," *IEEE Trans. Intrumentation and Measurement*, vol. 57, pp. 438–443, February 2008.

[135] C. Fager, K. Hausmair, K. Buisman, K. Andersson, E. Sienkiewicz, and D. Gustafsson, "Analysis of nonlinear distortion in phased array transmitters," in *2017 Integrated Nonlinear Microwave and Millimetre-wave Circuits Workshop (INMMiC)*, April 2017.

[136] Z. Dunn, M. Yeary, C. Fulton, and R. Rincon, "Impedance-dependent wideband digital predistortion of solid-state radar amplifiers," *IEEE Transactions on Aerospace and Electronic Systems*, vol. 53, pp. 2290–2303, October 2017.

[137] G. Montoro, P. L. Gilabert, E. Bertran, A. Cesari, and J. A. Garcia, "An LMS-based adaptive predistorter for cancelling nonlinear memory effects in RF power amplifiers," in *2007 Asia-Pacific Microwave Conference*, December 2007.

[138] Y. H. Lim, Y. S. Cho, I. W. Cha, and D. H. Youn, "An adaptive nonlinear prefilter for compensation of distortion in nonlinear systems," *IEEE Trans. on Signal Processing*, vol. 46, June 1998.

[139] A. D. Poularikas, *Adaptive Filtering*. Boca Raton, Florida: CRC Press, 2015.

[140] A. E. Abdelrahman, O. Hammi, A. K. Kwan, A. Zerguine, and F. M. Ghannouchi, "A novel weighted memory polynomial for behavioral modeling and digital predistortion of nonlinear wireless transmitters," *IEEE Trans. on Industrial Electronics*, vol. 63, pp. 1745–1753, October 2015.

[141] V. N. Manyam, D.-K. G. Pham, C. Jabbour, and P. Desgreys, "An FIR memory polynomial predistorter for wideband RF power amplifiers," in *2017 15th IEEE International New Circuits and Systems Conference (NEWCAS)*, June 2017.

[142] Z. A. Khan, E. Zenteno, P. Handel, and M. Isaksson, "Digital predistortion for joint mitigation of I/Q imbalance and MIMO power amplifier distortion," *IEEE Trans. Microwave Theory and Techniques*, vol. 65, pp. 322–333, January 2017.

[143] S. Lee, M. Kim, Y. Sirl, E.-R. Jeong, S. Hong, S. Kim, and Y. H. Lee, "Digital predistortion for power amplifiers in hybrid MIMO systems with antenna subarrays," in *2015 IEEE 81st Vehicular Technology Conference (VTC-Spring)*, May 2015.

[144] L. Liu, W. Chen, L. Ma, and H. Sun, "Single-PA-feedback digital predistortion for beamforming MIMO transmitter," in *2016 IEEE International Conference on Microwave and Millimeter Wave Technology (ICMMT)*, June 2016.

[145] H. Yan and D. Cabric, "Digital predistortion for hybrid precoding architecture in millimeter-wave massive MIMO systems," in *2017 IEEE International Conference on Acoustics, Speech and Signal Processing (ICASSP)*, March 2017.

[146] X. Liu, Q. Zhang, W. Chen, H. Feng, L. Chen, F. M. Ghannouchi, and Z. Feng, "Beam-oriented digital predistortion for 5G massive MIMO hybrid beamforming transmitters," *IEEE Trans. Microwave Theory and Techniques*, vol. 66, pp. 3419–3432, July 2018.

[147] N. Tervo, M. E. Leinonen, J. Aikio, T. Rahkonen, and A. Parssinen, "Analyzing the effects of pa variations on the performance of phased array digital predistortion," in *2018 IEEE 29th Annual International Symposium on Personal, Indoor and Mobile Radio Communications (PIMRC)*, September 2018.

[148] "Analog devices lays foundation for 4g to 5G migration with expanded radioverse wireless technology and design ecosystem." Analog Devices, June 2017.

[149] M. Grimm, M. Allen, J. Marttila, M. Valkama, and R. Thoma, "Joint mitigation of nonlinear RF and baseband distortions in wideband direct-conversion receivers," *IEEE Trans. Microwave Theory and Techniques*, vol. 62, pp. 166–182, January 2014.

[150] M. Grimm, R. K. Sharma, M. Hein, R. S. Thoma, and R. Zemmari, "Improved BER performance in GSM by mitigating non-linear distortions in the receiver," in *Proc. European Microwave Conference*, October 2013.

[151] R. Gharpurey, "Linearity enhancement techniques in radio receiver front-ends," *IEEE Trans. Circuits and Systems*, vol. 59, pp. 1667–1679, August 2012.

[152] E. Rebeiz and D. Cabric, "How wideband receiver nonlinearities impact spectrum sensing," in *Proc. IEEE Global Conference on Signal and Information Processing (GlobalSIP)*, December 2013.

[153] Y. Li, J. M. Rabaey, and A. Sangiovanni-Vincentelli, "Analysis of interference effects in MB-OFDM UWB systems," in *Proc. IEEE Wireless Communications and Networking Conference (WCNC)*, April 2008.

[154] *Standard for Information technology Telecommunications and information Exchange between Systems Local and metropolitan area networks Specific requirements - Part 15.3: Wireless Medium Access Control (MAC) and Physical Layer (PHY) Specifications for High Rate Wireless Personal Area Networks (WPANs)*. IEEE 802.16m, 2003.

[155] A. Taparugssanagorn, K. Umebayashi, J. Lehtomaki, and C. Pomalaza-Raez, "Analysis of the effect of nonlinear low noise amplifier with memory for wideband spectrum sensing," in *1st International Conference on 5G for Ubiquitous Connectivity*, November 2014.

[156] D. Dupleich, M. Grimm, F. Schlembach, and R. S. Thoma, "Practical aspects of a digital feedforward approach for mitigating non-linear distortions in receivers," in *Proc. 11th International Telecommunications in Modern Satellite, Cable and Broadcast Services Conference (TELSIKS)*, October 2013.

[157] P.-Y. Qin, Y. J. Guo, S. Member, and A. R. Weily, "A pattern reconfigurable u-slot antenna and its applications in MIMO systems," *IEEE Trans. Antennas Propag.*, vol. 60, no. 2, pp. 516–528, 2012.

[158] Z. Li, E. Ahmed, A. M. Eltawil, S. Member, and B. A. Cetiner, "A beam-steering reconfigurable antenna for WLAN applications," *IEEE Trans. Antennas Propag.*, vol. 63, no. 1, pp. 24–32, 2015.

[159] M. A. Hossain, I. Bahceci, and B. A. Cetiner, "Parasitic layer-based radiation pattern reconfigurable antenna for 5G communications," *IEEE Trans. Antennas Propag.*, vol. 65, no. 12, pp. 6444–6452, 2017.

[160] S. Zhang, G. H. Huff, J. Feng, and J. T. Bernhard, "A pattern reconfigurable microstrip parasitic array," *IEEE Transactions on Antennas and Propagation*, vol. 52, no. 10, pp. 2773–2776, 2004.

[161] A. Towfiq, S. Member, I. Bahceci, S. Blanch, J. Romeu, L. Jofre, B. A. Cetiner, and S. Member, "A reconfigurable antenna with beam steering and beamwidth variability for wireless communications," *IEEE Trans. Antennas Propag.*, vol. 66, no. 10, pp. 5052–5063, 2018.

[162] S. F. Bass, B. M. Hennessy, L. M. Szolc, and J. E. Ruyle, "Analysis of circularly polarized annular slot antennas to determine reconfiguration mechanism," in *2014 Antenna Applications Symposium*, September 2014.

[163] S. F. Bass, L. M. Szolc, and J. E. Ruyle, "Investigation of pattern reconfigurability using three-element loaded slot array," in *2015 Antenna Applications Symposium*, September 2015.

[164] N. H. Chamok, M. H. Yilmaz, H. Arslan, and M. Ali, "High-gain pattern reconfigurable MIMO antenna array for wireless handheld terminals," *IEEE Transactions on Antennas and Propagation*, vol. 64, no. 10, pp. 4306–4315, 2016.

[165] Y. F. Cheng, X. Ding, W. Shao, M. X. Yu, and B. Z. Wang, "A novel wide-angle scanning phased array based on dual-mode pattern-reconfigurable elements," *IEEE Antennas and Wireless Propagation Letters*, vol. 16, no. c, pp. 396–399, 2017.

[166] J. Butler and R. Rowe, "Beamforming matrix simplifies design of electronically scanned antennas," *Electron*, vol. 9, pp. 170–173, 1961.

[167] W. Li, C. Chu, K. Lin, and S. Chang, "Switched-beam antenna based on modified butler matrix with low sidelobe level," *IET Electronics Letters*, vol. 40, no. 5, pp. 4–5, 2004.

[168] J. Remez and R. Carmon, "Compact Designs of Waveguide Butler Matrices," *IEEE Trans. Antennas Propag.*, vol. 5, no. c, pp. 27–31, 2006.

[169] P. Chen, W. Hong, S. Member, Z. Kuai, J. Xu, H. Wang, J. Chen, H. Tang, J. Zhou, and K. Wu, "A multibeam antenna based on substrate integrated waveguide technology for MIMO wireless communications," *IEEE Trans. Antennas Propag.*, vol. 57, no. 6, pp. 1813–1821, 2009.

[170] B. Cetinoneri, S. Member, Y. A. Atesal, S. Member, and G. M. Rebeiz, "An 8×8 butler matrix in 0.13-μm CMOS for 5–6-GHz multibeam applications," *IEEE Trans. Microw. Theory Tech.*, vol. 59, no. 2, pp. 295–301, 2011.

[171] K. Wincza and S. Gruszczynski, "Miniaturized broadband 4×4 butler matrix designed with the use of quasi-lumped coupled-line couplers," *2012 8th Int. Caribbean Conf. on Devices, Circuits and Systems*, pp. 6–9, 2012.

[172] F. Wang and H. Wang, "A broadband compact low-loss 4×4 butler matrix in CMOS with stacked transformer based quadrature couplers," *2016 IEEE MTT-S Int. Microw. Symp.*, pp. 4–7, 2016.

[173] L. Zhang, A. Natarajan, and H. Krishnaswamy, "Scalable spatial notch suppression in spatio-spectral-filtering MIMO receiver arrays for digital beamforming," *IEEE Journal of Solid-State Circuits*, vol. 51, no. 12, pp. 3152–3166, 2016.

[174] L. Zhang and H. Krishnaswamy, "A 0.1-to-3.1 GHz 4-element MIMO receiver array supporting analog/RF arbitrary spatial filtering," *IEEE International Solid-State Circuits Conference*, pp. 410–412, February 2017.

[175] L. Zhang and H. Krishnaswamy, "Recent advances in analog/RF interference mitigation for massive MIMO receivers," *2017 IEEE 60th Int. MWSCAS*, pp. 21–24, August 2017.

[176] S. Jain, Y. Wang, and A. Natarajan, "A 10GHz CMOS RX frontend with spatial cancellation of co-channel interferers for MIMO/digital beamforming arrays," *Digest of Papers - IEEE Radio Frequency Integrated Circuits Symposium*, vol. 2016-July, pp. 99–102, 2016.

[177] N. Oshima, M. Kitsunezuka, K. Tsukamoto, and K. Kunihiro, "A 30-MHz 3-GHz CMOS array receiver with frequency and spatial interference filtering for adaptive multi-antenna systems," *IEEE Trans. Microw. Theory Tech.*, vol. 65, no. 2, pp. 362–373, 2017.

[178] D. Murphy, H. Darabi, A. Abidi, A. A. Hafez, A. Mirzaei, M. Mikhemar, and M. C. F. Chang, "A blocker-tolerant, noise-cancelling receiver suitable for wideband wireless applications," *IEEE Journal of Solid-State Circuits*, vol. 47, no. 12, pp. 2943–2963, 2012.